

5/22/56  
JLH

WCLSW

zhr

NACA TN 3674

# NATIONAL ADVISORY COMMITTEE FOR AERONAUTICS

TECHNICAL NOTE 3674

THEORETICAL PRESSURE DISTRIBUTIONS FOR SOME SLENDER  
WING-BODY COMBINATIONS AT ZERO LIFT

By Paul F. Byrd

Ames Aeronautical Laboratory  
Moffett Field, Calif.

**DISTRIBUTION STATEMENT A**  
Approved for Public Release  
Distribution Unlimited



Washington  
April 1956

Reproduced From  
Best Available Copy

20000515 119

M00-08-2340

G

NATIONAL ADVISORY COMMITTEE FOR AERONAUTICS

---

TECHNICAL NOTE 3674

---

THEORETICAL PRESSURE DISTRIBUTIONS FOR SOME SLENDER  
WING-BODY COMBINATIONS AT ZERO LIFT

By Paul F. Byrd

SUMMARY

Pressure distributions are calculated for some symmetrical wing-body combinations at zero lift. The theory of the calculations is based on the assumption of extremely slender wings and bodies and yields results for both subsonic and supersonic speeds. The examples considered are swept wings of constant chord mounted on bodies of nearly cylindrical form.

Of particular interest is the effect of indenting the body on the distribution of pressure over the wing. When the indentation is such as to maintain a constant total area of the cross sections normal to the stream, the theoretical pressure disturbances remain small throughout the transonic range. With such indentation the isobars tend to remain smooth and nearly parallel to the sweep of the wing surface.

INTRODUCTION

In several papers, important extensions to the Munk-Jones slender-body theory (refs. 1 and 2) for lifting wings and bodies have been made to include the theoretical effects of thickness on the aerodynamics of wings and wing-body combinations. Ward (ref. 3), solving the linearized differential equation for the perturbation velocity potential by operational methods, and employing asymptotic expansion of the solution, investigated the flow around bodies of general cross section at supersonic flight speeds. By a different procedure, similar results for a wing, body, or wing-body combination at subsonic speeds have been developed by Heaslet and Lomax (refs. 4 and 5). An analysis for subsonic flow was also carried out independently by Adams and Sears (ref. 6) who, in addition, made an extension for not-so-slender wings. Confining themselves to wings at zero angle of attack, Keune (ref. 7) and Oswatitsch and Keune (ref. 8) have recently obtained a slender-body theory that is slightly different from those of references 4, 5, and 6. In a more recent report,

---

<sup>1</sup>Supersedes NACA RM A54JO7 by Paul F. Byrd, 1954.

---

Harder and Klunker (ref. 9) have applied the basic ideas of the slender-body approximation to the nonlinear transonic equation for the velocity potential.

The principal object of the present investigation is to apply the general method of reference 4 in calculating the pressure distribution for some special cases of nonlifting slender wing-body combinations in subsonic and supersonic flow. The wing of the combinations is swept back and has a symmetrical section with rounded leading edges. Determination is made of the pressure for the wing alone and for cases when the wing is mounted on a circular cylinder or combined with a body indented such that the axial variation of cross-sectional area of the combination is constant. The effects of Mach number and sweep angle are included in the results presented.

#### LIST OF IMPORTANT SYMBOLS

$b_0$	value of $x$ at which $s_0 = s(x)$
$c_0$	root chord
$c_p$	pressure coefficient, $\frac{-2u}{U_0}$
$\tilde{c}_p$	pressure coefficient on indented wing-body combination
$l_0$	over-all length of the wing
$m$	slope of wing leading edge (See sketch (f).)
$M$	free-stream Mach number
$r$	polar distance in $y, z$ plane $\left(\sqrt{y^2 + z^2}\right)$
$\text{Re}$	real part of a complex quantity
$R_0$	radius of cylindrical portion of body
$R(x)$	radius of indented body of revolution
$\text{sgn}(x-\xi)$	sign of $(x-\xi)$
$s_0$	maximum value of $s(x)$
$s(x)$	local semispan
$S(x)$	local cross-sectional area of wing alone

$t(x)$	spanwise distance from $x$ axis to wing trailing edge
$u$	perturbation velocity in the $x$ direction
$U_0$	velocity of free stream
$v$	perturbation velocity in the $y$ direction
$v_r$	radial component of velocity in $yz$ plane
$w$	perturbation velocity in the $z$ direction
$x, y, z$	Cartesian coordinates ( $x$ downstream, $y$ to starboard, $z$ upward)
$\beta$	$\sqrt{ M^2 - 1 }$
$\theta$	polar angle in $yz$ plane
$\lambda(x, y)$	slope of wing surface in $x$ direction
$\phi$	perturbation velocity potential
$\phi_2$	part of potential satisfying $\phi_{yy} + \phi_{zz} = 0$
$\zeta$	complex variable ( $y + iz$ )
$\zeta_1$	complex variable ( $y_1 + iz_1$ )
$\tau$	constant related to $\tau_0$
$\tau_0$	maximum thickness of wing section

## Subscripts

$B$	body
$l$	lower surface of the wing ( $z = 0$ plane)
sub	subsonic
sup	supersonic
$u$	upper surface of the wing ( $z = 0$ plane)
$W$	wing

## ANALYSIS

The thickness distribution of a symmetrical wing is prescribed. Under the restriction that the thickness is small and that the configuration is slender, formulas to be applied later (see "Applications" section) will now be briefly presented for determining the pressure coefficients for particular nonlifting wing-body combinations. Equations are first given for the wing without a body, and are then modified for cases when the wing is mounted on a circular cylinder or on an indented body of revolution.

## Nonlifting Wing Alone

The differential equation and boundary conditions.- Expressed in terms of the perturbation potential  $\phi(x,y,z)$ , the basic linearized partial differential equation for subsonic as well as supersonic flow is the familiar Prandtl-Glauert equation

$$(1 - M_0^2)\phi_{xx} + \phi_{yy} + \phi_{zz} = 0 \quad (1)$$

where  $M_0$  is the free-stream Mach number. If the surface of a wing  $z(x,y)$  is given, solutions to the differential equation must satisfy the boundary condition that the flow is parallel to the wing surface. When the wing is thin, it is sufficient to satisfy this requirement in the plane  $z = 0$ . Analytically, the expression of the condition is

$$\left(\frac{\partial \phi}{\partial z}\right)_{z=+0} = w_u(x,y) = U_0 \frac{\partial z_u}{\partial x} = U_0 \lambda_u(x,y) \quad (2)$$

where  $U_0$  is the free-stream velocity and  $w_u(x,y)$  is the vertical induced velocity on the upper side of the  $z = 0$  plane.

Velocity potential.- When the flow is supersonic, the formula for the perturbation potential subject to the boundary condition (2) is known to be (e.g., see ref. 10)

$$\phi(x,y,z) = -\frac{1}{\pi} \frac{\partial}{\partial x} \int \int_T w_u(\xi, \eta) \operatorname{arccosh} \frac{x - \xi}{\beta \sqrt{(y - \eta)^2 + z^2}} d\xi d\eta \quad (3)$$

where the region of integration  $T$  is the portion of the plan form lying within the Mach forecone from the point  $x, y, z$ . In the case of subsonic flow fields, the solution of the differential equation (1) may be expressed in the form

$$\phi(x, y, z) = -\frac{1}{2\pi} \frac{\partial}{\partial x} \iint_T w_u(\xi, \eta) \operatorname{arcsinh} \frac{x - \xi}{\beta \sqrt{(y - \eta)^2 + z^2}} d\xi d\eta \quad (4)$$

with  $T$  now extending over the entire plan form. These two solutions yield the potential due to a distribution of sources of strength proportional to the slope of the wing surface  $\lambda_u(x, y)$ .

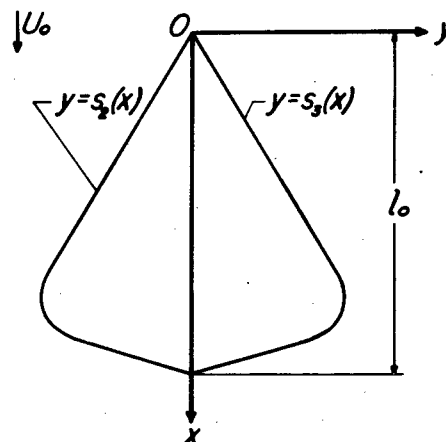
When the wing is slender, that is, if  $\frac{\beta \sqrt{(y - \eta)^2 + z^2}}{x - \xi}$  is considered very small, further approximations to the linearized potential (3) and (4) can be readily made. In this event, one may employ the approximate relations

$$\left. \begin{aligned} \operatorname{arccosh} \frac{x - \xi}{\beta \sqrt{(y - \eta)^2 + z^2}} &\approx \ln \frac{2(x - \xi)}{\beta \sqrt{(y - \eta)^2 + z^2}} \\ \operatorname{arcsinh} \frac{x - \xi}{\beta \sqrt{(y - \eta)^2 + z^2}} &\approx \operatorname{sgn}(x - \xi) \ln \frac{2|x - \xi|}{\beta \sqrt{(y - \eta)^2 + z^2}} \end{aligned} \right\} \quad (5)$$

where the symbol  $\operatorname{sgn}(x - \xi)$  means that the sign of  $(x - \xi)$  is to be taken.

Consider now a thin pointed wing of symmetrical section with straight or sweptforward trailing edges as is shown in sketch (a). Use of the relations (5) in equations (3) and (4) then gives the result (ref. 4)

$$\phi(x, y, z) = \phi_2(x, y, z) + g(x) \quad (6)$$



Sketch (a)

where

$$\Phi_2(x, y, z) = \frac{U_0}{2\pi} \int_{s_2(x)}^{s_3(x)} \lambda_u(x, \eta) \ln [(y - \eta)^2 + z^2] d\eta \quad (7)$$

and

$$g(x) = -\frac{U_0}{2\pi} \frac{\partial}{\partial x} \int_0^x S'(\xi) \ln \frac{2(x - \xi)}{\beta} d\xi \quad (8a)$$

for supersonic flow, and

$$g(x) = -\frac{U_0}{4\pi} \frac{\partial}{\partial x} \int_0^{l_0} \operatorname{sgn}(x - \xi) S'(\xi) \ln \frac{2|x - \xi|}{\beta} d\xi \quad (8b)$$

for subsonic flow. The function  $S'(x)$ , the derivative of the cross-sectional area of the wing in a  $yz$  plane, is found from

$$S'(x) = 2 \frac{d}{dx} \int_{s_2(x)}^{s_3(x)} z_u(x, \eta) d\eta \quad (9)$$

It is seen from equation (6) that the slender-body approximation to the linearized supersonic and subsonic potentials consists of two parts. The first part ( $\Phi_2$ ) in each case is independent of Mach number and is a harmonic function in the transverse plane; that is, it satisfies the two-dimensional Laplace equation

$$\Phi_{yy} + \Phi_{zz} = 0 \quad (10)$$

The second part ( $g$ ) depends on the cross-sectional area of the wing and is a function of  $x$  and  $\beta$  only.

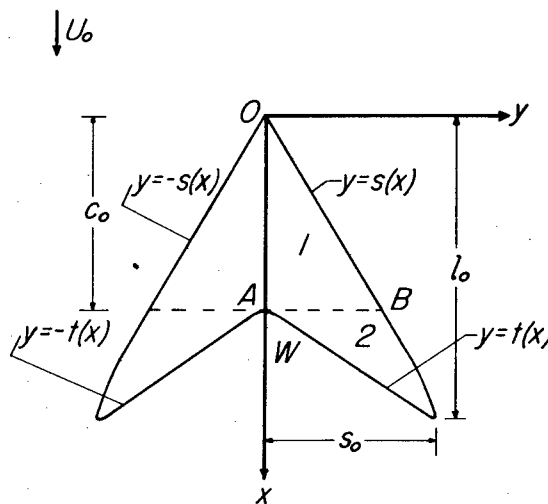
Inspection of equations (6) and (8) shows that the value of the potential for a particular wing at some Mach number  $M_1$  can be written in terms of the potential given at another Mach number  $M_0$ . Thus

$$\left. \begin{aligned} \varphi_{\text{sup}\beta_1} &= \varphi_{\text{sup}\beta_0} + \frac{U_0}{2\pi} S'(x) \ln \frac{\beta_1}{\beta_0} \\ \varphi_{\text{sub}\beta_1} &= \varphi_{\text{sub}\beta_0} + \frac{U_0}{2\pi} S'(x) \ln \frac{\beta_1}{\beta_0} \end{aligned} \right\} \quad (11a)$$

with  $\beta_1 = \sqrt{M_1^2 - 1}$  and  $\beta_0 = \sqrt{M_0^2 - 1}$ . The supersonic and subsonic potentials may also be related. If one has already found an expression for the supersonic potential, he can then obtain the subsonic potential by means of the equation

$$\varphi_{\text{sub}} = \varphi_{\text{sup}} + \frac{U_0}{2\pi} S'(x) \ln \frac{\beta_{\text{sub}}}{\beta_{\text{sup}}} + \frac{U_0}{4\pi} \int_0^{l_0} \frac{S'(\xi)}{x - \xi} d\xi \quad (11b)$$

Certain symmetrical wings whose trailing edges are swept back as in sketch (b) can also be treated by the simplified theory, provided the chordwise variation in shape of the cross sections is sufficiently smooth and gradual that the assumption of two-dimensional transverse flow may reasonably be applied. Since the wing is at zero angle of attack and the flow is symmetrical about the  $xy$  plane, the source distribution  $\lambda_u(x, y)$  in the plane of the wing in region  $W$  between the axis and the trailing edge is set equal to zero. If the limits of integration are properly adjusted, equation (6) will then formally still apply and yield expressions for the potential in the two regions 1 and 2 of the sketch. Thus for region 1, in the  $z = 0$  plane, one obtains



Sketch (b)

$$\varphi_{\text{sup}} = \frac{U_0}{\pi} \int_0^s \lambda_u(x, \eta) \ln |y^2 - \eta^2| d\eta -$$

$$\frac{U_0}{2\pi} \frac{\partial}{\partial x} \int_0^x S_1'(\xi) \ln \frac{2}{\beta} (x - \xi) d\xi, \quad (x \leq c_0) \quad (12a)$$



and in region 2

$$\begin{aligned} \Phi_{\text{sup}} = & \frac{U_0}{\pi} \int_t^s \lambda_u(x, \eta) \ln |y^2 - \eta^2| d\eta - \frac{U_0}{2\pi} \frac{\partial}{\partial x} \int_0^{c_0} S_1'(\xi) \ln(x - \xi) d\xi - \\ & \frac{U_0}{2\pi} \frac{\partial}{\partial x} \int_{c_0}^x S_2'(\xi) \ln \frac{2}{\beta} (x - \xi) d\xi, \quad (x \geq c_0) \end{aligned} \quad (12b)$$

where

$$\left. \begin{aligned} S_1'(x) &= 4 \frac{d}{dx} \int_0^{s(x)} z_u(x, \eta) d\eta, & 0 \leq x \leq c_0 \\ S_2'(x) &= 4 \frac{d}{dx} \int_{t(x)}^{s(x)} z_u(x, \eta) d\eta, & c_0 \leq x \leq l_0 \end{aligned} \right\} \quad (13)$$

The subsonic solution is obtained from the supersonic solution by using equation (11b).

Pressure coefficient.- After determining the potential for a wing from the equations in the foregoing section, the pressure on the surface of the wing is found by differentiation. The pressure coefficient is related to the perturbation velocities by the equation (ref. 4)

$$c_p(x, y, 0) = - \left[ \frac{2}{U_0} \frac{\partial \Phi}{\partial x} + \frac{1}{U_0^2} \left( \frac{\partial \Phi}{\partial y} \right)^2 + \frac{1}{U_0^2} \left( \frac{\partial \Phi}{\partial z} \right)^2 \right]_{z=0} \quad (14a)$$

which is an approximation to the complete Bernoulli equation consistent with both the linearized differential equation (1) and the assumption of slenderness. For planar problems, further simplification achieved by neglecting the nonlinear terms  $(\partial \Phi / \partial y)^2$  and  $(\partial \Phi / \partial z)^2$  yields satisfactory estimates for the coefficient.

Thus

$$c_p(x, y, 0) = -\frac{2}{U_0} \left( \frac{\partial \Phi}{\partial x} \right)_{z=0} \quad (14b)$$

where  $\Phi$  is obtained from equations (11b) and (12).

It should be pointed out, however, that equations (11b), (12), and (14) will not furnish realistic results for the pressures<sup>1</sup> for a wing in either subsonic or supersonic flow unless certain restrictions are imposed on the gradient of cross-sectional area and its derivative  $S''(x)$ . Consider, for example, the pressure found along the line AB where regions 1 and 2 in sketch (b) join. In supersonic flow, one finds from equations (12) and (14b) that at this line there is a jump  $\Delta c_p$  in the pressure coefficient given by

$$\Delta c_p = c_{p1} - c_{p2} = \frac{1}{\pi} \lim_{\epsilon \rightarrow 0} \left\{ \Delta S''(c_0) \ln \frac{2\epsilon}{\beta \sqrt{s^2(c_0) - y^2}} + 4 \left[ \frac{dt}{dx} \lambda_u(x, t) \right]_{c_0 + \epsilon} \ln \frac{2\epsilon}{\beta y} \right\} \quad (15)$$

where

$$\Delta S''(c_0) = S_1''(c_0) - S_2''(c_0)$$

and where the usual assumption that  $S'(0) = S'(c_0) = 0$  has been made. Evidently, along the line AB a logarithmic singularity will occur in the pressure distribution in going from region 1 to region 2 if  $S_1''(c_0) \neq S_2''(c_0)$ . (The infinity would of course be higher than logarithmic if  $\Delta S''(c_0)$  is singular.) The formulas for the pressure coefficients presented in this report and in reference 4 are therefore good only for cases where the plan form and the slope of the wing surface are sufficiently smooth so that there are no abrupt changes in either  $S'$  or  $S''$ . (This holds true also for the formulas given in references 3, 6, and 7. The restriction on  $S''$ , however, may be somewhat relaxed in employing the slender-body theory of reference 8.)

---

<sup>1</sup>Although the theory may give spurious infinite pressures on certain portions of the wing, the results obtained for the wave drag by integrating the product of pressure and surface slope over the wing may be finite and reasonable.

---

Even if there is no jump in the pressure coefficient at the line AB, the slope of the pressure curve may not be continuous. It can be shown, for instance, that a singularity will occur in the slope of the curve for the pressure coefficient in case  $S'''(c_0)$  is discontinuous.

### Wing on a Cylindrical Body

The equations presented in the foregoing sections for the wing alone will now be modified to yield formulas for calculating the pressure dis-

tribution on a combination composed of a symmetrical wing  $z_u(x,y) = -z_l(x,y)$  mounted on an infinite circular cylinder having radius  $R_0$  (see sketch (c)). The surface of the wing chosen here will also be considered symmetrical about the  $xz$  plane, but the method applies equally well if this is not the case. The procedure followed is essentially the same if the fuselage is any body of revolution instead of a circular cylinder.

In studying such combinations, it is usually convenient to introduce a second coordinate system. Let the  $yz$  plane be represented by a complex variable

$$\zeta = y + iz = re^{i\theta} \quad (16)$$

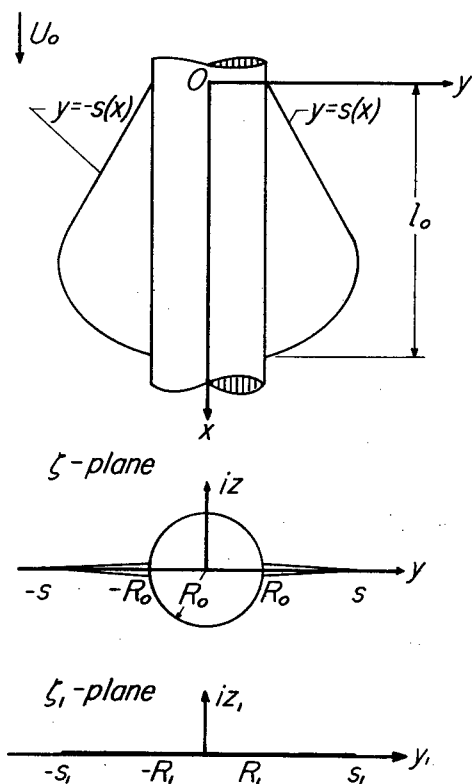
and then consider a  $\zeta_1$  plane

$$\zeta_1 = y_1 + iz_1 = r_1 e^{i\theta_1}$$

obtained from the  $\zeta$  plane by the Joukowski transformation

$$\zeta_1 = \zeta + \frac{R_0^2}{\zeta} \quad (17)$$

The transformation (17) maps the  $\zeta$  plane onto the  $\zeta_1$  plane so that a circle representing a section of the body in the  $\zeta$  plane is mapped onto a portion of the real axis in the  $\zeta_1$  plane, while the part of the real axis outside the circle is transformed into an adjoining part of the real axis of the  $\zeta_1$  plane. (See sketch (c).) It can easily be shown from the equation that the geometric relations



Sketch (c)

$$\left. \begin{aligned}
 R_1 &= 2R_0 \\
 y_1 &= y + \frac{R_0^2}{y}, & y_1^2 &\geq R_1^2 \\
 y_1 &= 2R_0 \cos \theta, & y_1^2 &\leq R_1^2 \\
 s_1 &= s + \frac{R_0^2}{s}
 \end{aligned} \right\} \quad (18)$$

hold for  $z_1$  equal to zero.

The technique employed is to transform the boundary conditions from the  $\xi$  plane to the  $\xi_1$  plane and to find a solution in the latter plane. The solution is then transformed back to the physical plane for the completion of the problem.

Perturbation velocity potential at the wing surface.- A consequence of the conformal transformation is that the complex velocities in the two planes  $\xi$  and  $\xi_1$  are related by the equation

$$v - iw = (v_1 - iw_1) \frac{d\xi_1}{d\xi} \quad (19)$$

or, in polar coordinates (ref. 11),

$$\left. \begin{aligned}
 v &= v_1 \left[ 1 - \left( \frac{R_0}{r} \right)^2 \cos 2\theta \right] + w_1 \left( \frac{R_0}{r} \right)^2 \sin 2\theta \\
 w &= w_1 \left[ 1 - \left( \frac{R_0}{r} \right)^2 \cos 2\theta \right] - v_1 \left( \frac{R_0}{r} \right)^2 \sin 2\theta \\
 v_r &= \left[ v_1 \cos \theta + w_1 \sin \theta \right] \left[ 1 - \left( \frac{R_0}{r} \right)^2 \right] + 2w_1 \left( \frac{R_0}{r} \right)^2 \sin \theta
 \end{aligned} \right\} \quad (19a)$$

From these equations it follows that the boundary conditions in the  $z_1 = 0$  plane are

$$\left. \begin{aligned} w_1 &= \frac{v_r}{2 \sin \theta} = \frac{U_0(dR_0/dx)}{2 \sin \theta} = 0, & y_1^2 < R_1^2 \\ w_1 &= \frac{w}{1 - R_0^2/y^2}, & R_1^2 < y_1^2 \leq s_1^2 \end{aligned} \right\} \quad (20)$$

with  $w$  related to the streamwise slope of the wing surface by equation (2).

The two-dimensional solution  $\phi_2$  in the  $\xi_1$  plane at  $z_1 = 0$  is, from equation (7),

$$\phi_2(x, y_1, 0) = \frac{1}{\pi} \int_{-s_1}^{s_1} w_1(x, \eta_1) \ln |y_1 - \eta_1| d\eta_1 \quad (21)$$

Putting now

$$\eta_1 = \eta + \frac{R_0^2}{\eta}$$

and using relations (18) and the boundary conditions (20), one finally has for equation (21)

$$\phi_2(x, y) = \frac{U_0}{\pi} \int_{R_0}^{s(x)} \lambda_u(x, \eta) \ln \left| \frac{(y^2 - \eta^2)(y^2 \eta^2 - R_0^4)}{y^2 \eta^2} \right| d\eta \quad (22)$$

If one of the functions  $g$  given by formulas (8) is then added to this equation for  $\phi_2$ , the velocity potential on the wing may be obtained for either supersonic or subsonic flow. Thus, for the supersonic perturbation potential on the upper surface, there results

$$\begin{aligned} \phi_{\text{sup}} &= \frac{U_0}{\pi} \int_{R_0}^{s(x)} \lambda_u(x, \eta) \ln \left| \frac{(y^2 - \eta^2)(y^2 \eta^2 - R_0^4)}{y^2 \eta^2} \right| d\eta - \\ &\quad \frac{U_0}{2\pi} \frac{\partial}{\partial x} \int_0^x S'(\xi) \ln \frac{2}{\beta} (x - \xi) d\xi \end{aligned} \quad (23)$$

and for the subsonic potential

$$\varphi_{\text{sub}} = \frac{U_0}{\pi} \int_{R_0}^{s(x)} \lambda_u(x, \eta) \ln \left| \frac{(y^2 - \eta^2)(y^2 \eta^2 - R_0^4)}{y^2 \eta^2} \right| d\eta -$$

$$\frac{U_0}{4\pi} \frac{\partial}{\partial x} \int_0^{l_0} \text{sgn}(x - \xi) S'(\xi) \ln \frac{2}{\beta} |x - \xi| d\xi \quad (24)$$

Pressure coefficient at the wing surface.— The pressure coefficients on the surface of the wing of the combination are obtained by differentiating equations (23) and (24) with respect to  $x$  and then employing relation<sup>2</sup> (14b). Thus

$$c_{p\text{sup}} = -\frac{2}{\pi} \frac{\partial}{\partial x} \int_{R_0}^{s(x)} \lambda_u(x, \eta) \ln \left| \frac{(y^2 - \eta^2)(y^2 \eta^2 - R_0^4)}{y^2 \eta^2} \right| d\eta +$$

$$\frac{1}{\pi} \frac{\partial^2}{\partial x^2} \int_0^x S'(\xi) \ln \frac{2}{\beta} (x - \xi) d\xi \quad (25a)$$

and

$$c_{p\text{sub}} = -\frac{2}{\pi} \frac{\partial}{\partial x} \int_{R_0}^{s(x)} \lambda_u(x, \eta) \ln \left| \frac{(y^2 - \eta^2)(y^2 \eta^2 - R_0^4)}{y^2 \eta^2} \right| d\eta +$$

$$\frac{1}{2\pi} \frac{\partial^2}{\partial x^2} \int_0^{l_0} \text{sgn}(x - \xi) S'(\xi) \ln \frac{2}{\beta} |x - \xi| d\xi \quad (25b)$$

or, with the aid of equation (11b),

$$c_{p\text{sub}} = c_{p\text{sup}} - \frac{1}{\pi} S''(x) \ln \frac{\beta_{\text{sub}}}{\beta_{\text{sup}}} - \frac{1}{2\pi} \frac{\partial}{\partial x} \int_0^{l_0} \frac{S'(\xi)}{x - \xi} d\xi \quad (26)$$

---

<sup>2</sup>As in the case of planar problems, the squared terms in the pressure relation can be neglected in considering a combination whose body is a circular cylinder. (See ref. 4.)

---

The coefficient for a particular wing at some Mach number  $M_1$ , written in terms of the coefficient at another Mach number  $M_0$ , is

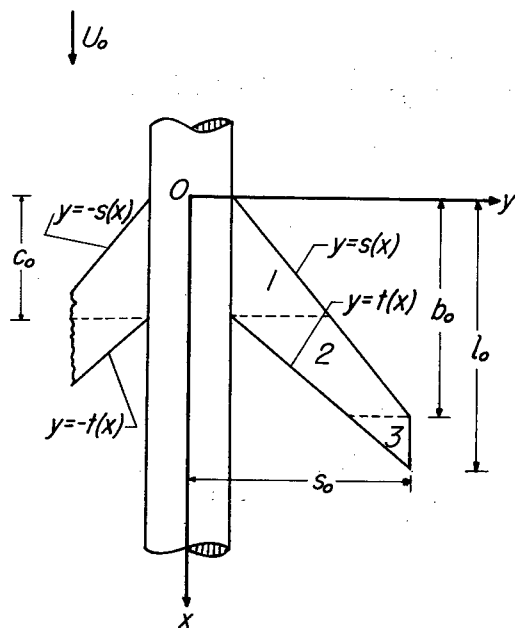
$$c_{p_{\text{sup}}\beta_1} = c_{p_{\text{sup}}\beta_0} + \frac{1}{\pi} S''(x) \ln \frac{\beta_0}{\beta_1} \quad (27a)$$

and

$$c_{p_{\text{sub}}\beta_1} = c_{p_{\text{sub}}\beta_0} + \frac{1}{\pi} S''(x) \ln \frac{\beta_0}{\beta_1} \quad (27b)$$

where  $\beta_1 = \sqrt{|M_1^2 - 1|}$  and  $\beta_0 = \sqrt{|M_0^2 - 1|}$ .

It should be noted that formulas (25a) and (25b) are not uniformly valid for all values of  $R_0$ . If the radius  $R_0$  is equal to zero, the



Sketch (d)

equations reduce immediately to those given previously for the wing without a body. As the radius approaches infinity, however, one finds that formulas (25a) and (25b) yield a value of the pressure coefficient that differ from the results for the wing alone by a term equal to  $\frac{S''(x)}{\pi} \ln \frac{1}{2}$ . Employing the equations for values of  $R_0$  that are large violates the assumption of slenderness according to the approximate theory used herein.

When the wing mounted on the combination is swept back, as shown in sketch (d), the slope  $\lambda_u(x, \eta)$  is taken equal to zero in the gap between the trailing edge and the body. The formulas obtained in regions 1, 2, and 3 for the supersonic pressure coefficient on the upper surface of the wing are then as follows:

Region 1:

$$c_{p_1} = -\frac{2}{\pi} \frac{\partial}{\partial x} \int_{R_0}^{s(x)} \lambda_u(x, \eta) \ln \left| \frac{(y^2 - \eta^2)(y^2 \eta^2 - R_0^4)}{y^2 \eta^2} \right| d\eta +$$

$$\frac{1}{\pi} \frac{\partial^2}{\partial x^2} \int_0^x S_1'(\xi) \ln \frac{2}{\beta} (x - \xi) d\xi, \quad (0 \leq x \leq c_0)$$

Region 2:

$$c_{p2} = -\frac{2}{\pi} \frac{\partial}{\partial x} \int_{t(x)}^{s(x)} \lambda_u(x, \eta) \ln \left| \frac{(y^2 - \eta^2)(y^2 \eta^2 - R_0^4)}{y^2 \eta^2} \right| d\eta +$$

$$\frac{1}{\pi} \frac{\partial^2}{\partial x^2} \int_0^{c_0} S_1'(\xi) \ln(x - \xi) d\xi + \frac{1}{\pi} \frac{\partial^2}{\partial x^2} \int_{c_0}^x S_2'(\xi) \ln \frac{2}{\beta} (x - \xi) d\xi$$

$$(c_0 \leq x \leq b_0) \quad (28b)$$

Region 3:

$$c_{p3} = -\frac{2}{\pi} \frac{\partial}{\partial x} \int_{t(x)}^{s_0} \lambda_u(x, \eta) \ln \left| \frac{(y^2 - \eta^2)(y^2 \eta^2 - R_0^4)}{y^2 \eta^2} \right| d\eta +$$

$$\frac{1}{\pi} \frac{\partial^2}{\partial x^2} \int_0^{c_0} S_1'(\xi) \ln(x - \xi) d\xi + \frac{1}{\pi} \frac{\partial^2}{\partial x^2} \int_{c_0}^{b_0} S_2'(\xi) \ln(x - \xi) d\xi +$$

$$\frac{1}{\pi} \frac{\partial^2}{\partial x^2} \int_{b_0}^x S_3'(\xi) \ln \frac{2}{\beta} (x - \xi) d\xi, \quad (b_0 \leq x \leq l_0) \quad (28c)$$

where  $b_0$  is the value of  $x$  at which  $s_0 = s(x)$ . Use of the relation (26) in conjunction with the above three formulas will furnish equations for the pressure coefficient in subsonic flow in the various regions.

#### Wing on an Indented Body

In the previous formulas for the pressure distribution attributable to thickness, the coefficient becomes infinite<sup>3</sup> when the Mach number approaches unity because the formulas contain a term involving  $S'(x) \ln \frac{2}{\beta}$ .

It is thus possible to construct slender configurations which will give a theoretically finite pressure coefficient even at the speed of sound. Under the assumptions of slender-body theory, this may be achieved if the gradient of cross-sectional area of the configuration in a  $yz$  plane vanishes identically. Combinations constructed in this manner on an

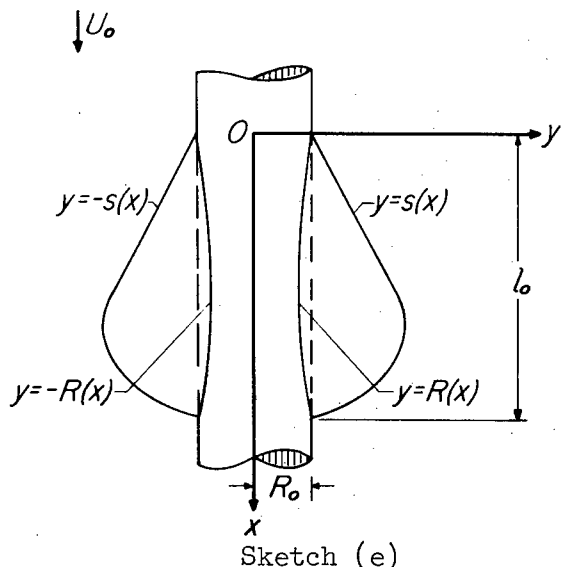
---

<sup>3</sup>This of course is not a property of slender-body theory alone. Except in particular cases, steady-state linearized theory also in general yields infinite pressures at  $\beta = 0$ .



infinitely long fuselage are slightly indented in the vicinity of the wing and possess, according to the theory, the important property of having zero wave drag.

Velocity potential at the wing surface.— Let the surface  $z_u(x, y) = -z_l(x, y)$  of a symmetrical wing be specified and assume that the indented fuselage is a body of revolution which deviates slightly from a basic circular cylinder of radius  $R_0$ . The cross-sectional area  $S(x)$  of the exposed wing is then given by



$$S(x) = 4 \int_{R(x)}^{s(x)} z_u(x, \eta) d\eta \quad (29)$$

where  $R$  is the radius of the indented body. (See sketch (e).) In order for the streamwise gradient of cross-sectional area of the entire combination to be zero, the relation

$$\pi R^2(x) = \pi R_0^2 - S(x), \quad S(x) \ll \pi R_0^2 \quad (30a)$$

or

$$2\pi R \frac{dR}{dx} = -S'(x) \quad (30b)$$

must hold. Since the quantity  $S(x)$  is known from formula (29), equation (30a) can thus be solved for the radius  $R$  of the body.

Now the perturbation potential in the  $\xi_1$  plane at  $z_1 = 0$  has the form

$$\varphi_2(x, y_1, 0) = \frac{1}{\pi} \int_{-s_1}^{s_1} w_1(x, \eta_1) \ln |y_1 - \eta_1| d\eta_1 \quad (31a)$$

or

$$\varphi_2(x, y_1, 0) = \frac{1}{\pi} \int_{-r_1}^{r_1} w_1(x, \eta_1) \ln |y_1 - \eta_1| d\eta_1 + \frac{1}{\pi} \int_{r_1}^{s_1} w_1(x, \eta_1) \ln |y_1^2 - \eta_1^2| d\eta_1 \quad (31b)$$

with

$$s_1 = s + \frac{R^2}{s}, \quad y_1 = y + \frac{R^2}{y}, \quad r_1 = 2R \quad (32)$$

The term corresponding to the  $g(x)$  of equations (8), which is to be added to this  $\phi_2$ , is zero since there is no change in the cross-sectional area of the specified shape of the  $yz$  plane.

From the last relation in equation (19a) it follows (upon putting  $R$  in place of  $R_0$ ) that in the interval  $\eta_1^2 < r_1^2$  the boundary condition may be expressed

$$w_1 = \frac{v_r}{2 \sin \theta} = \frac{(dR/dx)U_0}{2\sqrt{1 - (\eta_1/r_1)^2}}; \quad r = R \quad (33)$$

For very thin wings, and for deviation  $R_0 - R$  of the same order as the wing thickness, the condition in the interval  $r_1^2 < \eta_1^2 < s_1^2$  is approximately

$$w_1 = \frac{w}{1 - R^2/\eta^2} = \frac{U_0(\partial z_u/\partial x)}{1 - R^2/\eta^2} \quad (34)$$

Making use of equation (33), one can then write the first term on the right in equation (31b) as

$$\frac{1}{\pi} \int_{-r_1}^{r_1} w_1(x, \eta_1) \ln |y_1 - \eta_1| d\eta_1 = U_0 R \frac{dR}{dx} \ln y, \quad y^2 \geq R^2 \quad (35)$$

where, from equation (30b), the quantity  $R(dR/dx)$  may be replaced by  $-1/2\pi$  times the gradient of cross sectional area  $S'(x)$  of the wing. In the second integral in equation (31b), set

$$\eta_1 = \eta + \frac{R^2}{\eta}$$

and use relations (34). The final form for the velocity potential at the upper surface of the wing thus becomes

$$\phi(x, y, 0) = -\frac{U_0}{2\pi} S'(x) \ln y +$$

$$\frac{U_0}{\pi} \int_R^s \lambda_u(x, \eta) \ln \left| \frac{(y^2 - \eta^2)(y^2 \eta^2 - R^4)}{y^2 \eta^2} \right| d\eta, \quad y \geq R \quad (36)$$

Formula (36) for the velocity potential for a slender combination whose body is indented according to the area rule (ref. 12) is evidently independent of Mach number and therefore holds (within the assumptions of the simplified theory) for subsonic, transonic, and supersonic speeds. If the limits of integration are adjusted, the equation may also be used for combinations with sweptback wings.

Pressure coefficient at the wing surface.- On the surface of the wing the pressure coefficient can be found from relation (14a), that is,

$$c_{p_W} = - \left[ \frac{2}{U_0} \frac{\partial \phi}{\partial x} + \frac{1}{U_0^2} \left( \frac{\partial \phi}{\partial y} \right)^2 \right]_{z=0} - \left( \frac{\partial z_u}{\partial x} \right)^2 \quad (37)$$

where the potential  $\phi$  is obtained from equation (36).

#### APPLICATIONS

The formulas which were given the preceeding part of this report will now be applied for the purpose of performing detailed calculations of the pressure distribution for some particular nonlifting combinations having a symmetrical wing with constant chord.

##### Wing Mounted on a Body of Circular Cross Section

Pressure coefficient on the surface of the wing.- The wing of the combination<sup>4</sup> considered here is mounted on a circular cylinder and has an upper surface defined by

$$z_u(x, y) = \tau(c_0 m - s + y) \sqrt{(s - y)(c_0 m - s + y)} \quad (38)$$

with

$$s = mx + R_0$$

$$z_u(x, y) = z_u(x, -y) = -z_l(x, y) = -z_l(x, -y)$$

and

$$\tau = \frac{8\tau_0}{3m^2 c_0^2 \sqrt{3}} \quad (39)$$

---

<sup>4</sup>This combination will be referred to as the basic combination.

the constant  $\tau_0$  being the maximum thickness. The profile resembles a Joukowski section and is the same for all values of  $y$ . On the starboard side of the wing, the slope of the surface is given by the relation

$$\frac{\partial z_u}{\partial x} = \lambda_u(x, y) = \frac{w_u(x, y)}{U_0} = \frac{m\tau}{2} (c_0 m - 4s + 4y) \sqrt{\frac{c_0 m - s + y}{s - y}} \quad (40)$$

From this equation it is seen that the slope possesses a square-root infinity at the leading edge and is zero at the trailing edge.

The gradient of cross-sectional area of the wing is

$$S_1'(x) = 4\tau m^3 (c_0 - x) \sqrt{x(c_0 - x)} = 4m z_u(x, R_0), \quad (0 \leq x \leq c_0) \quad (41a)$$

in region 1 in sketch (f) and is

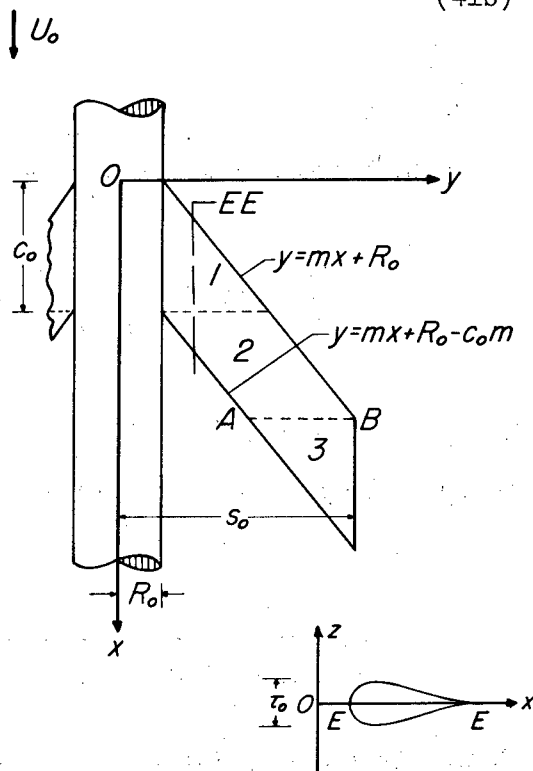
$$S_2'(x) \equiv 0, \quad c_0 \leq x \leq (s_0 - R_0)/m \quad (41b)$$

in region 2; for region 3,

$$S_3'(x) = -4m z_u(x, s_0), \quad (s_0 - R_0)/m \leq x \leq (s_0 - R_0 + c_0 m)/m \quad (41b)$$

Since  $S''$  is not continuous across the line AB, the approximate theory employed here will give unrealistic results in the regions of the tips. In calculating the pressures for the wing-body combination, attention will therefore be confined to regions 1 and 2 only. The calculations to be given in subsonic flow will be based on the assumption that the tips are located far downstream and have no effect on the other two regions.

Use of the equations (40) and (41) in formulas (28a) and (28b) yields the following final results for the supersonic pressure coefficient on the upper surface of the wing for regions 1 and 2:



Sketch (f)

Region 1:

$$c_{p\text{sup}} = \frac{m^2 \tau}{\pi} \left[ 16R_0 \tan^{-1} \sqrt{\frac{x}{c_0 - x}} + 2m(c_0 - 4x) \sqrt{\frac{c_0 - x}{x}} \ln \frac{8xy(c_0 - x)}{\beta c_0(y^2 - R_0^2)} + \right. \\ \left. F(x, y) + F(x, -y) - 2F(x, 0) + F\left(x, \frac{R_0^2}{y}\right) + F\left(x, -\frac{R_0^2}{y}\right) \right], \\ (0 \leq x \leq c_0) \quad (42a)$$

Region 2:

$$c_{p\text{sup}} = m^2 \tau \left[ 8R_0 + 2m(4x - c_0) \sqrt{\frac{x - c_0}{x}} + 2(4s - c_0 m) \sqrt{\frac{s - c_0 m}{s}} + \right. \\ (c_0 m - 4s - 4y) \sqrt{\frac{s - c_0 m + y}{s + y}} + \left( c_0 m - 4s + 4 \frac{R_0^2}{y} \right) \sqrt{\frac{s - c_0 m - R_0^2/y}{s - R_0^2/y}} + \\ \left. \left( c_0 m - 4s - 4 \frac{R_0^2}{y} \right) \sqrt{\frac{s - c_0 m + R_0^2/y}{s + R_0^2/y}} \right] \\ (c_0 \leq x, s - c_0 m < y < x; s = mx + R_0) \quad (42b)$$

where

$$F(x, \eta) = (c_0 m - 4s - 4\eta) \sqrt{\frac{s - c_0 m + \eta}{s + \eta}} \\ \left[ \frac{\pi}{2} - \tan^{-1} \frac{(c_0 - x)(2s + \eta) - (\eta x + R_0 c_0)}{2 \sqrt{x(c_0 - x)(s + \eta)(s - c_0 m + \eta)}} \right] \quad (43a)$$

when  $c_0 m - s - \eta < 0$ , and

$$F(x, \eta) = (c_0 m - 4s - 4\eta) \sqrt{\frac{c_0 m - s - \eta}{s + \eta}} \\ \ln \frac{c_0(\eta + R_0)}{(c_0 - x)(2s + \eta) - (\eta x + R_0 c_0) + \sqrt{x(c_0 - x)(s + \eta)(c_0 m - s - \eta)}} \quad (43b)$$

when  $c_0 m - s - \eta > 0$

It is seen from equation (26) that the formulas for the pressure coefficient in subsonic flow can be obtained by adding two terms to the above equations for the supersonic pressure coefficient. Since the value of  $S'$  in region 2 is identically zero, the terms to be added for region 1 become

$$-\frac{1}{2\pi} \frac{\partial}{\partial x} \int_0^{c_0} \frac{S'(\xi)}{x - \xi} d\xi = \tau m^3 [4x - 3c_0], \quad (x \leq c_0) \quad (44a)$$

and for region 2

$$-\frac{1}{2\pi} \frac{\partial}{\partial x} \int_0^{c_0} \frac{S'(\xi)}{x - \xi} d\xi = \tau m^3 \left[ 4x - 3c_0 + (c_0 - 4x) \sqrt{\frac{x - c_0}{x}} \right], \quad (x \geq c_0) \quad (44b)$$

The subsonic pressure coefficient on the upper surface of the wing can therefore be written in region 1 as

$$c_{p_{sub}} = c_{p_{sup}} + \frac{m^3 \tau}{\pi} \left[ \pi(4x - 3c_0) + 2(4x - c_0) \sqrt{\frac{c_0 - x}{x}} \ln \frac{\beta_{sub}}{\beta_{sup}} \right] \quad (45a)$$

and in region 2 as

$$c_{p_{sub}} = c_{p_{sup}} + m^3 \tau \left[ 4x - 3c_0 + (c_0 - 4x) \sqrt{\frac{x - c_0}{x}} \right] \quad (45b)$$

where  $c_{p_{sup}}$  is given by equations (42).

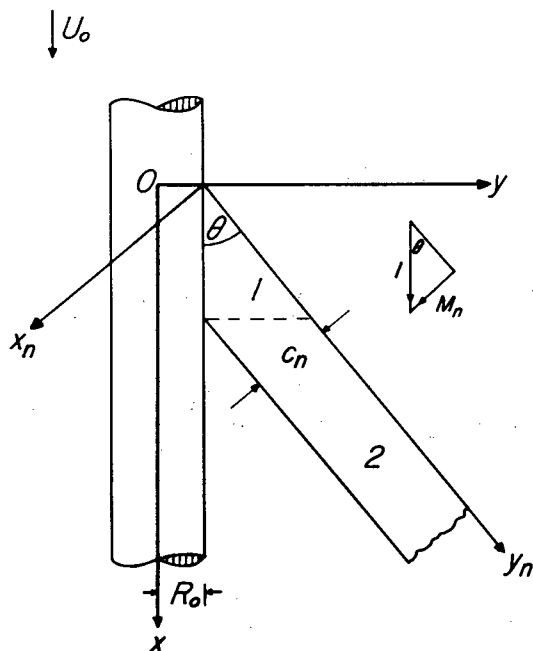
Formulas (42) and (45), which give the pressure coefficients on the wing of the combination indicated in sketch (f), will be plotted and the results discussed in a later section. An obvious result noted now is that in region 2 the formulas do not depend on Mach number for either supersonic or subsonic flow, but that the subsonic coefficient in this region is always greater than the supersonic coefficient because the inequality

$$m^3 \tau \left[ 4x - 3c_0 + (c_0 - 4x) \sqrt{\frac{x - c_0}{x}} \right] > 0 \quad (46)$$

holds for all values  $x \geq c_0$ .

As a check, let us now consider the asymptotic behavior of equations (38), (42b), and (45b) far outboard along the wing. For this purpose, we introduce a change in coordinate system by means of the transformation

$$\left. \begin{aligned} x &= x_n \sin \theta + y_n \sin \theta \\ y - R_0 &= -x_n \cos \theta + y_n \sin \theta \end{aligned} \right\} \quad (47a)$$



(See sketch (g).) Setting  $\tan \theta = m$ , one can then write

$$\left. \begin{aligned} x &= \frac{mx_n + y_n}{\sqrt{1 + m^2}} \\ y - R_0 &= \frac{my_n - x_n}{\sqrt{1 + m^2}} \\ x_n &= \frac{mx - (y - R_0)}{\sqrt{1 + m^2}} \\ y_n &= \frac{x + m(y - R_0)}{\sqrt{1 + m^2}} \end{aligned} \right\} \quad (47b)$$

Sketch (g)

and

$$\left. \begin{aligned} c_n &= c_0 m / \sqrt{1 + m^2} \\ M_n &= m / \sqrt{1 + m^2} \\ U_n &= U_0 m / \sqrt{1 + m^2} \\ \beta_n &= 1 / \sqrt{1 + m^2} \end{aligned} \right\} \quad (48)$$

Equation (38) thus becomes

$$z_n = \frac{8\tau_0}{3\sqrt{3}c_n^2} (c_n - x_n)^{3/2} (x_n)^{1/2}$$

which agrees with the approximate equation employed in two-dimensional section theory for a thin Joukowski base profile of thickness ratio  $\frac{4\tau_0}{3\sqrt{3}c_n}$ . (See ref. 13.) The pressure coefficient for such a two-dimensional airfoil is

$$c_p = -\frac{2}{U_n} \frac{\partial \phi}{\partial x_n} = -\frac{8\tau_0}{3\sqrt{3}c_n \beta_n} \left[ 3 - 4 \left( \frac{x_n}{c_n} \right) \right] \quad (49a)$$

or, written in terms of the  $xy$  system,

$$c_p = -\frac{8\tau_0}{3\sqrt{3}c_0^2} [3c_0 m - 4(mx - y + R_0)] \quad (49b)$$

This equation is in agreement with the asymptotic expression of the pressure coefficient for region 2 obtained far outboard along the wing from either equation (42b) or (45b).

Pressure coefficient on the body.—The formula for determining the pressure coefficient on the surface of the body is (ref. 4)

$$c_{p_B} = - \left[ \frac{2}{U_0} \frac{\partial \phi}{\partial x} + \frac{1}{U_0^2 R^2} \left( \frac{\partial \phi}{\partial \theta} \right)^2 \right]_B - \left( \frac{dR}{dx} \right)^2 \quad (50a)$$

When the body is a circular cylinder, this relation reduces to

$$c_{p_B} = -\frac{2}{U} \left( \frac{\partial \phi}{\partial x} \right)_B \quad (50b)$$

It is apparent that application of equation (50b) requires a knowledge of the value of the potential  $\phi$  in space, so that formulas (28), which hold for  $z = 0$ , must be "analytically continued." One way that will in effect accomplish this is as follows:

Set

$$\zeta = y + iz = R_0 e^{i\theta}$$

and form the function

$$\Phi(x, \zeta, 0) = \phi(x, \zeta, 0) + i\psi(x, \zeta, 0) \quad (51)$$



where  $\phi(x, \xi, 0)$  is taken from equations (23) and (24), with the function  $\psi$  defined by<sup>5</sup>

$$\psi(x, \xi, 0) = \int_{\xi}^{s(x)} w_u(x, \eta) d\eta \quad (52)$$

The constructed function (51) will obviously satisfy Laplace's equation in the  $yz$  plane; and it can be verified without difficulty that the boundary condition  $v_r = 0$  is also satisfied. The coefficient on the body can then be calculated from the formula

$$c_p = - \frac{2}{U_0} \operatorname{Re} \left( \frac{\partial \phi}{\partial x} \right) \quad (53)$$

where the symbol  $\operatorname{Re}$  means that the real part is to be taken.

For region 1, the final result obtained for the pressure coefficient on the body in supersonic flow for the basic combination considered in this part of the report is

$$c_{p_{\text{sup}}} = \frac{m^2 \tau}{\pi} \left\{ 16R_0 \tan^{-1} \sqrt{\frac{x}{c_0 - x}} - 2F(x, 0) + F(x, R_0 e^{i\theta}) + \right. \\ \left. F(x, R_0 e^{-i\theta}) + F(x, -R_0 e^{i\theta}) + F(x, -R_0 e^{-i\theta}) + \right. \\ \left. \operatorname{Re} \left[ 2m(c_0 - 4x) \sqrt{\frac{c_0 - x}{x}} \ln \frac{8x(c_0 - x)e^{i\theta}}{\beta c_0 (e^{2i\theta} - 1)R_0} - \right. \right. \\ \left. \left. i\pi(c_0 m - 4s + 4R_0 e^{i\theta}) \sqrt{\frac{c_0 m - s + R_0 e^{i\theta}}{s - R_0 e^{i\theta}}} \right] \right\} \quad (x \leq c_0) \quad (54a)$$

where the function  $F(x, \eta)$  is given by equations (43). The result found for the supersonic pressure coefficient in region 2 can be put in the form

---

<sup>5</sup>An arbitrary real function  $E(x)$  may, in general, be added to the right side of equation (52). Such a function, however, would in no way affect the real part of  $\partial \phi / \partial x$ , since  $iE$  is purely imaginary.

---

$$\begin{aligned}
c_{p_{sup}} = m^2 \tau & \left[ 8R_0 + 2m(4x - c_0) \sqrt{\frac{x - c_0}{x}} + 2(4s - c_0 m) \sqrt{\frac{s - c_0 m}{s}} + \right. \\
& (c_0 m - 4s - 4R_0 e^{i\theta}) \sqrt{\frac{s + R_0 e^{i\theta} - c_0 m}{s + R_0 e^{i\theta}}} + \\
& (c_0 m - 4s - 4R_0 e^{-i\theta}) \sqrt{\frac{s + R_0 e^{-i\theta} - c_0 m}{s + R_0 e^{-i\theta}}} + \\
& (c_0 m - 4s + 4R_0 e^{i\theta}) \sqrt{\frac{s - R_0 e^{i\theta} - c_0 m}{s - R_0 e^{i\theta}}} + \\
& \left. (c_0 m - 4s + 4R_0 e^{-i\theta}) \sqrt{\frac{s - R_0 e^{-i\theta} - c_0 m}{s - R_0 e^{-i\theta}}} \right], \quad (x \geq c_0) \quad (54b)
\end{aligned}$$

Corresponding formulas for the pressure coefficient on the body in subsonic flow are obtained from the above two equations by adding to them the terms on the right of equations (44a) and (44b), respectively. For any fixed value of  $y$  in region 2, relations (45b) and (46) furnish the inequality

$$c_{p_{sub}} > c_{p_{sup}} \quad (55)$$

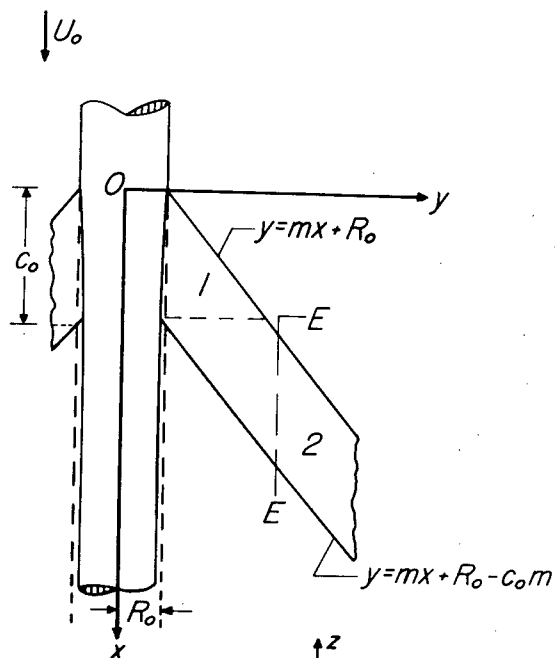
which, as mentioned before, is also true for the coefficients on the wing.

#### Wing Mounted on an Indented Body

The constant-chord wing whose thickness distribution on the starboard side is given by

$$\left. \begin{aligned}
z_u(x, y) &= \tau(c_0 m - s + y) \sqrt{(s - y)(c_0 m - s + y)}, \quad R(x) \leq y \leq s \\
s &= mx + R_0 \\
\tau &= \frac{8\tau_0}{3m^2 c_0^2 \sqrt{3}}
\end{aligned} \right\} \quad (56)$$

will now be combined with an indented body of revolution which deviates slightly from a basic cylinder in the manner that makes the local cross-sectional area of the configuration a constant. The wing has the same profile along EE as the one in the previous example. (See sketch (h).) Since the gradient of cross-sectional area of the combination is set equal to zero, the wave drag, according to the slender-body theory, is also zero.



Sketch (h)

The cross-sectional area of the wing in region 2 is equal to the constant

$$S_2(x) = 4 \int_{s=c_0 m}^s z_u(x, \eta) d\eta = \frac{c_0^3 m^3 \pi}{4} \quad (57)$$

and the radius of the indented body in this region is therefore the constant

$$R_2 = R_0 \sqrt{1 - \frac{S_2(x)}{\pi R_0^2}} = R_0 \sqrt{1 - \frac{c_0^3 m^3}{4 R_0^2}} \quad (58)$$

Corresponding equations for region 1 are

$$S_1(x) = 4 \int_{R_1}^s z_u(x, \eta) d\eta = \frac{\pi}{12} \left\{ 3m^3 c_0^3 \cos^{-1} \frac{c_0 m - 2s + 2R_1}{c_0 m} + 2[2(s - R_1)(7c_0 m - 4s + 4R_1) - 3c_0^2 m^2] \sqrt{(s - R_1)(c_0 m - s + R_1)} \right\} \quad (59)$$

and

$$R_1(x) = R_0 \sqrt{1 - \frac{S_1(x)}{\pi R_0^2}}; \quad 0 < R_2 \leq R_1 < R_0 \quad (60)$$

Equation (60), however, does not give an explicit value of the radius in region 1 because the function  $S_1$  itself involves  $R_1$ . Moreover, the function  $S_1$  is a transcendental function of  $R_1$ , so that equation (60) can only be solved by graphical or other methods of approximation. By means of the mean-value theorem, we can write the equation in the form

$$S_1(x) = S_{11}(x) + 4z_u(x,d)(R_0 - R_1) \quad (61)$$

where  $d$  is a certain value in the interval  $R_1 < d < R_0$ , and

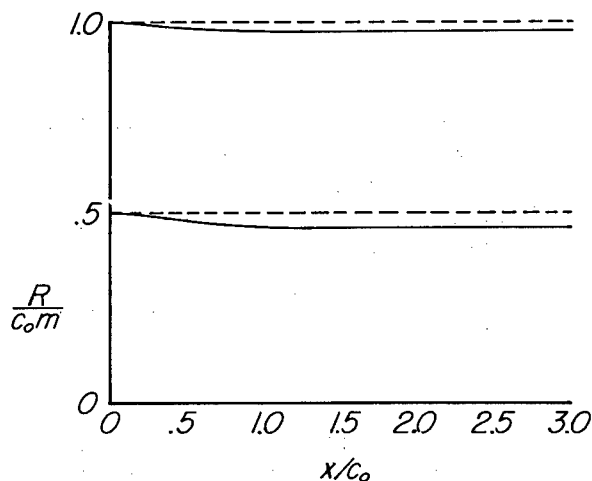
$$S_{11}(x) = \frac{m^3 \tau}{12} \left[ 2(14xc_0 - 8x^2 - 3c_0^2) \sqrt{x(c_0 - x)} + 3c_0^3 \cos^{-1} \frac{c_0 - 2x}{c_0} \right] \quad (62)$$

is the cross-sectional area of the wing in region 1 neglecting the additional area exposed by the indentation. Since the deviation  $R_0 - R_1$  is assumed to be of the same order as the wing thickness, neglect of the term  $4z_u(x,d)(R_0 - R_1)$  will evidently introduce only an error of the second order in thickness. For very thin wings, the radius  $R_1$  may thus be approximated by

$$R_1(x) = R_0 \sqrt{1 - \frac{S_{11}(x)}{\pi R_0^2}} \quad (63)$$

which is now an explicit function of  $x$ .

Sketch (i) indicates the variation of the radius as a function of  $x/c_0$  for  $\tau_0/mc_0$  equal to 0.1 and values of  $R_0/mc_0$  equal to 0.5 and 1.0.



Sketch (i)

Relations (14b) and (53) can be immediately employed for determining the pressure coefficient on the surface of the wing and on the body in region 2, because the portion of the body in that region is a circular cylinder. Use of these relations with equation (36), (57), and (58), then finally yields for the coefficient on the upper surface of the wing

$$\begin{aligned} \tilde{c}_{p_2} = m^2 \tau \left[ 2(4s - 3c_0m) + 2(4s - c_0m) \sqrt{\frac{s - c_0m}{s}} + (c_0m - 4s - 4y) \sqrt{\frac{s - c_0m + y}{s + y}} + \right. \\ \left. \left( c_0m - 4s + 4 \frac{R_2^2}{y} \right) \sqrt{\frac{s - c_0m - R_2^2/y}{s - R_2^2/y}} + \left( c_0m - 4s - 4 \frac{R_2^2}{y} \right) \sqrt{\frac{s - c_0m + R_2^2/y}{s + R_2^2/y}} \right] \\ (s - c_0m < y < s) \quad (64) \end{aligned}$$

and for the coefficient on the body

$$\begin{aligned} \tilde{c}_{p_2} = m^2 \tau \left[ 2(4s - 3c_0 m) + 2(4s - c_0 m) \sqrt{\frac{s - c_0 m}{s}} + (c_0 m - 4s - 4R_2 e^{i\theta}) \sqrt{\frac{s - c_0 m + R_2 e^{i\theta}}{s - R_2 e^{i\theta}}} + \right. \\ \left. (c_0 m - 4s - 4R_2 e^{-i\theta}) \sqrt{\frac{s - c_0 m + R_2 e^{-i\theta}}{s - R_2 e^{-i\theta}}} + (c_0 m - 4s + 4R_2 e^{i\theta}) \sqrt{\frac{s - c_0 m - R_2 e^{i\theta}}{s - R_2 e^{i\theta}}} + \right. \\ \left. (c_0 m - 4s + 4R_2 e^{-i\theta}) \sqrt{\frac{s - c_0 m - R_2 e^{-i\theta}}{s - R_2 e^{-i\theta}}} \right] \quad (65) \end{aligned}$$

These equations are employed for

$$x \geq c_0 - \frac{R_0}{m} + \sqrt{\frac{R_0^2}{m^2} - \frac{c_0^3 m \tau}{4}}$$

the equality sign giving the value of  $x$  at the trailing-edge fuselage junction. The two formulas do not involve Mach number and apply for subsonic, transonic, and supersonic flight speeds. Comparison of formula (64) with equations (42b) and (45b) shows that for a fixed  $y$  in region 2 the inequality

$$\tilde{c}_p > c_{p_{\text{sub}}} > c_{p_{\text{sup}}} \quad (66)$$

is satisfied when  $x \geq c_0$ . Values calculated in region 2 for the subsonic and supersonic pressure coefficients along a section on the surface of the wing of the basic combination will thus be less than the values obtained for the coefficient  $\tilde{c}_p$  on the wing surface of the indented combination.

In region 1, the body is not cylindrical but it is found that the squared terms in the pressure relation (37) may be neglected since they contribute only quantities involving the second and higher order in wing thickness that are small in comparison with  $-\frac{2}{U_0} \frac{\partial \phi}{\partial x}$ . Even the first term in relation (37) gives rise, for the particular combination considered, to some small terms of the second order. Such quantities, however, are also found to be negligible. The formulas to be presented here for the pressure coefficients in region 1 will therefore contain (like those for region 2) only terms of the same order as the thickness of the wing.

Use of equations (14b), (36), (53), (59), and (60) thus furnish the following final expressions for the pressure coefficients on the wing surface and on the body in region 1 of the combination in sketch (h):

$$\tilde{c}_{p1} = \frac{m^2 \tau}{\pi} \left[ 2(mc_0 - 4s + 4R_1) \sqrt{\frac{c_0 m - s + R_1}{s - R_1}} \ln \frac{y^2}{y^2 - R_1^2} - 8 \sqrt{(s - R_1)(c_0 m - s + R_1)} + \right.$$

$$\left. 4(4s - 3c_0 m) \tan^{-1} \sqrt{\frac{s - R_1}{c_0 m - s + R_1}} + F_1(x, y) + F_1(x, -y) - 2F_1(x, 0) + F_1\left(x, \frac{R_1^2}{y}\right) + F_1\left(x, -\frac{R_1^2}{y}\right) \right] \quad (67)$$

and

$$\tilde{c}_{p1} = \frac{m^2 \tau}{\pi} \left\{ -8 \sqrt{(s - R_1)(c_0 m - s + R_1)} + 4(4s - 3c_0 m) \tan^{-1} \sqrt{\frac{s - R_1}{c_0 m - s + R_1}} + F_1(x, R_1 e^{i\theta}) + F_1(x, R_1 e^{-i\theta}) - \right.$$

$$\left. 2F_1(x, 0) + F_1(x, -R_1 e^{i\theta}) + F_1(x, -R_1 e^{-i\theta}) + \operatorname{Re} \left[ 2(c_0 m - 4s + 4R_1) \sqrt{\frac{c_0 m - s + R_1}{s - R_1}} \ln \frac{e^{2i\theta}}{(e^{2i\theta} - 1)} - \right. \right.$$

$$\left. \left. i\pi(c_0 m - 4s + 4R_1 e^{i\theta}) \sqrt{\frac{c_0 m - s + R_1 e^{i\theta}}{s - R_1 e^{i\theta}}} \right] \right\} \quad (68)$$

where for  $c_0 m - s + \eta > 0$

$$F_1(x, \eta) = (c_0 m - 4s + 4\eta) \sqrt{\frac{c_0 m - s + \eta}{s - \eta}} \ln \left[ \frac{mc_0(\eta - R_1)}{2s(c_0 m - s) + (2s - c_0 m)(\eta + R_1) - 2R_1 + 2 \sqrt{(s - \eta)(c_0 m - s + \eta)(s - R_1)(c_0 m - s + R_1)}} \right] \quad (69)$$

and for  $c_0 m - s + \eta < 0$

$$F_1(x, \eta) = (c_0 m - 4s + 4\eta) \sqrt{\frac{s - c_0 m - \eta}{s - \eta}} \left[ \frac{\pi}{2} - \tan^{-1} \frac{2s(c_0 m - s) + (2s - c_0 m)(\eta + R_1) - 2\eta R_1}{2 \sqrt{(s - \eta)(s - c_0 m - \eta)(s - R_1)(c_0 m - s + R_1)}} \right] \quad (70)$$

## NUMERICAL RESULTS AND DISCUSSION

Graphs of the pressure coefficients for a wing alone and for the two wing-body combinations in sketches (f) and (h) are shown in figures 1, 2, and 3. Figures 1 and 2 give plots for the coefficients along several spanwise stations of the basic combination ( $R_0/c_{0m} = 0.5$ ) for subsonic and supersonic flow at  $m\beta = 0.5$ , while figure 3 presents plots of the coefficient for the indented wing-body combination which are independent of Mach number. The plot in figure 4 gives the variation of the pressure on the body in the plane of the wing.

Figures 1 and 2 show that, except at the wing-fuselage juncture, the pressure coefficients have a finite negative<sup>6</sup> value at the leading edge and increase to finite positive values at the trailing edge. On sections which are cut by the plane  $x = c_0$  (i.e., passing through the trailing-edge fuselage juncture) the slopes of the curves are discontinuous. It is also apparent that the effect of the presence of the body on the coefficient does not extend very far downstream beyond the trailing-edge fuselage juncture; the difference between the calculations for the wing on the combination and those for the wing alone, for instance, are too small to show up in the plots for sections more than one chord length from the body.

In figure 3, the pressure coefficients for nearly all sections on the wing of the indented combination are very close to the curve for the two-dimensional wing. The discontinuity in the slope of the curve that was quite noticeable along sections such as BB of figures 1 and 2 is far less apparent in figure 3.

The graph in figure 5 is the function which, according to equations (27), can be added to the values given in figures 1 and 2 for the subsonic or supersonic pressure coefficient along the section AA and BB of the wing to yield values of the coefficient at other Mach numbers. (Sections CC, DD, and EE lie in region 2 where the coefficients do not depend on Mach number.) For example, the pressure  $\frac{c_p}{(\tau_0/c_0)_m}$  at the leading edge along BB in subsonic flow for  $m\beta = 0.4$  is, using figures 1 and 5 in conjunction with equations (27),  $-4.1 - 0.2 = -4.3$ .

Figure 6 shows isobaric charts of the pressure coefficients for the wing without body in subsonic and supersonic flow at  $m\beta = 0.5$ , and also

---

<sup>6</sup> The occurrence of a negative pressure at the nose of a Joukowski-like section is the result of the thin-airfoil simplification. A more accurate theory would show a small region of positive pressure (i.e., a stagnation point with the maximum value equal to the impact pressure of the component of stream velocity normal to the edge).

---

a chart giving the two-dimensional results. The figures 6(a) and 6(b) indicate that the pattern of the isobars in the region behind the trailing-edge fuselage juncture is essentially the same as the two-dimensional in figure 6(c), but that in the region near and upstream of the juncture, a marked deviation from the straight isobars of the two-dimensional case is evident.

Isobaric maps are also shown in figure 7 for the basic wing-body combination in subsonic and supersonic flow, and for the indented wing-body combination. Figures 7(a) and 7(b) illustrate that in the region downstream from the trailing-edge fuselage juncture (even near the juncture itself) the isobars are not much different from those for the wing alone, and that the body therefore has little effect in this region. In the region adjacent to the body, the pattern of the isobars is qualitatively similar to the case for the wing alone but the pressures are lower. A remarkable difference between the chart in figure 7(c) for the indented combination and those in figures 7(a) and 7(b) for the basic combination is that the isobaric pattern on the wing for the indented combination is essentially two-dimensional over practically the whole wing.

Examination of the three charts in figure 7 also indicate that the maximum negative pressure on the wing occurs at the leading edge near the boundary between regions 1 and 2. In fact, it can be shown that the maximum occurs at the boundary. In view of the inequality (66), indentation in accordance with the area rule reduces the maximum perturbation velocities on the wing.

Ames Aeronautical Laboratory  
National Advisory Committee for Aeronautics  
Moffett Field, Calif., Oct. 7, 1954

#### REFERENCES

1. Munk, Max. M.: The Aerodynamic Forces on Airship Hulls. NACA Rep. 184, 1924.
2. Jones, Robert T.: Properties of Low-Aspect-Ratio Pointed Wings at Speeds Below and Above the Speed of Sound. NACA Rep. 835, 1946. (Supersedes NACA TN 1032.)
3. Ward, G. N.: Supersonic Flow Past Slender Pointed Bodies. Quart. Mech. and Appl. Math., vol. II, pt. 1, 1949, pp. 75-97.
4. Heaslet, Max. A., and Lomax, Harvard: The Calculation of Pressure on Slender Airplanes in Subsonic and Supersonic Flow. NACA TN 2900, 1953.



5. Heaslet, Max. A., and Lomax, Harvard: Supersonic and Transonic Small Perturbation Theory. Section D., vol. 6, of High-Speed Aerodynamics and Jet Propulsion. Princeton University Press, 1954.
6. Adams, Mac. C., and Sears, William R.: Slender-Body Theory - Review and Extension. Jour. Aero. Sci., vol. 20, no. 2, Feb., 1953, pp. 85-98.
7. Keune, Friedrich: Low Aspect Ratio Wings with Small Thickness at Zero Lift in Subsonic and Supersonic Flow. Kungl. Tekniska Högskolan, Stockholm. Institutionen för Flygteknik. Tech. Note 21. June, 1952.
8. Oswatitsch, K., and Keune, F.: Nicht angestellte Körper kleiner Spannweite in Unter- und Überschallströmung. Zeitschrift für Flugwissenschaften, Bd. 1, Heft 6, Braunschweig, Nov. 1953.
9. Harder, Keith C. and Klunker, E. B.: On Slender-Body Theory at Transonic Speeds. NACA RM L54A29a, 1954.
10. Lomax, Harvard, Heaslet, Max. A., and Fuller, Franklyn B.: Integrals and Integral Equations in Linearized Wing Theory. NACA Rep. 1054, 1951. (Supersedes NACA TN 2252.)
11. Lomax, Harvard, and Byrd, Paul F.: Theoretical Aerodynamic Characteristics of a Family of Slender Wing-Tail-Body Combinations. NACA TN 2554, 1951.
12. Whitcomb, Richard T.: A Study of the Zero-Lift Drag-Rise Characteristics of Wing-Body Combinations Near the Speed of Sound. NACA RM L52H08, 1952.
13. Allen, H. Julian: General Theory of Airfoil Sections Having Arbitrary Shape or Pressure Distribution. NACA Rep. 833, 1945.

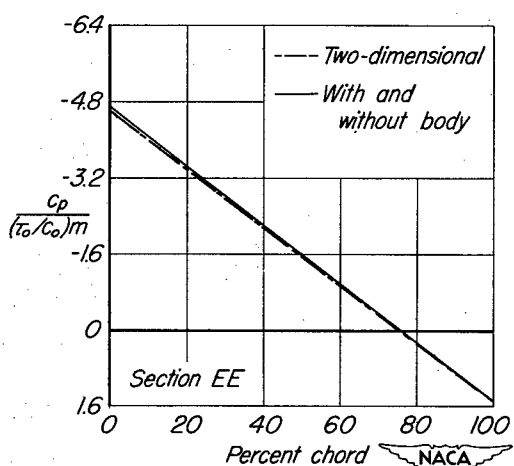
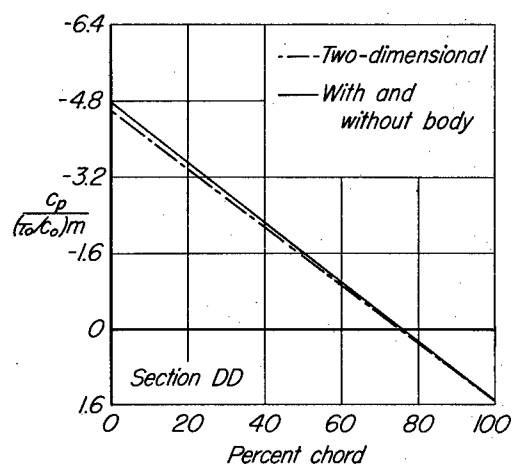
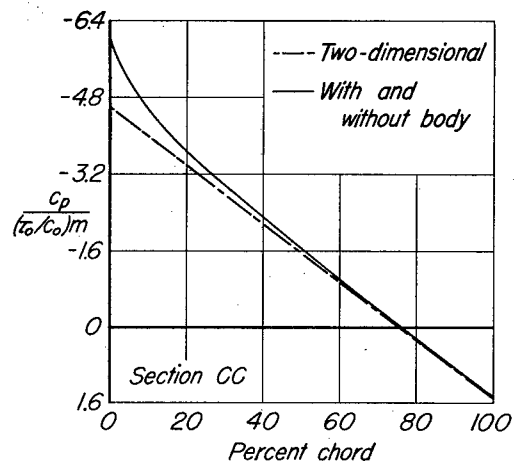
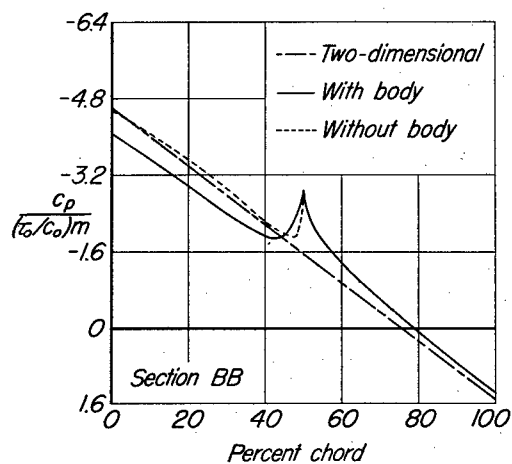
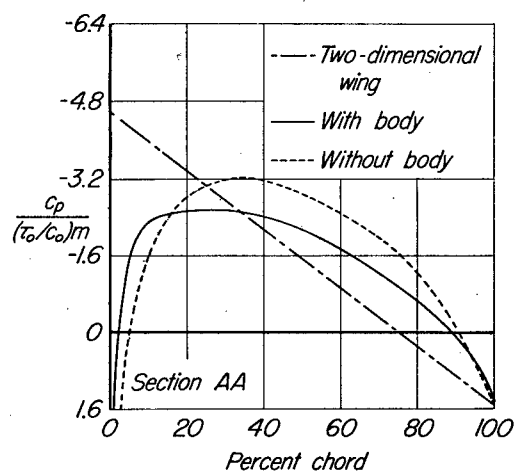
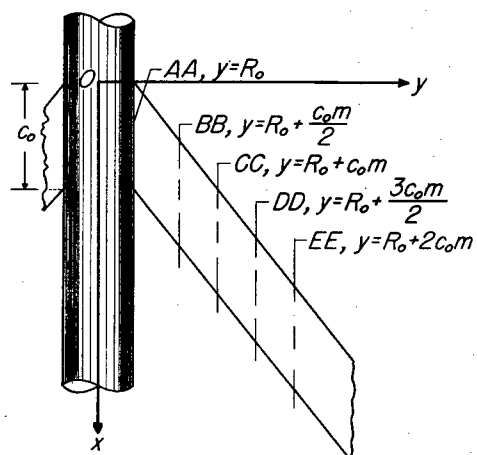


Figure 1.- Subsonic pressure coefficient on upper surface of wing of the basic combination;  $m\beta = 0.5$ .

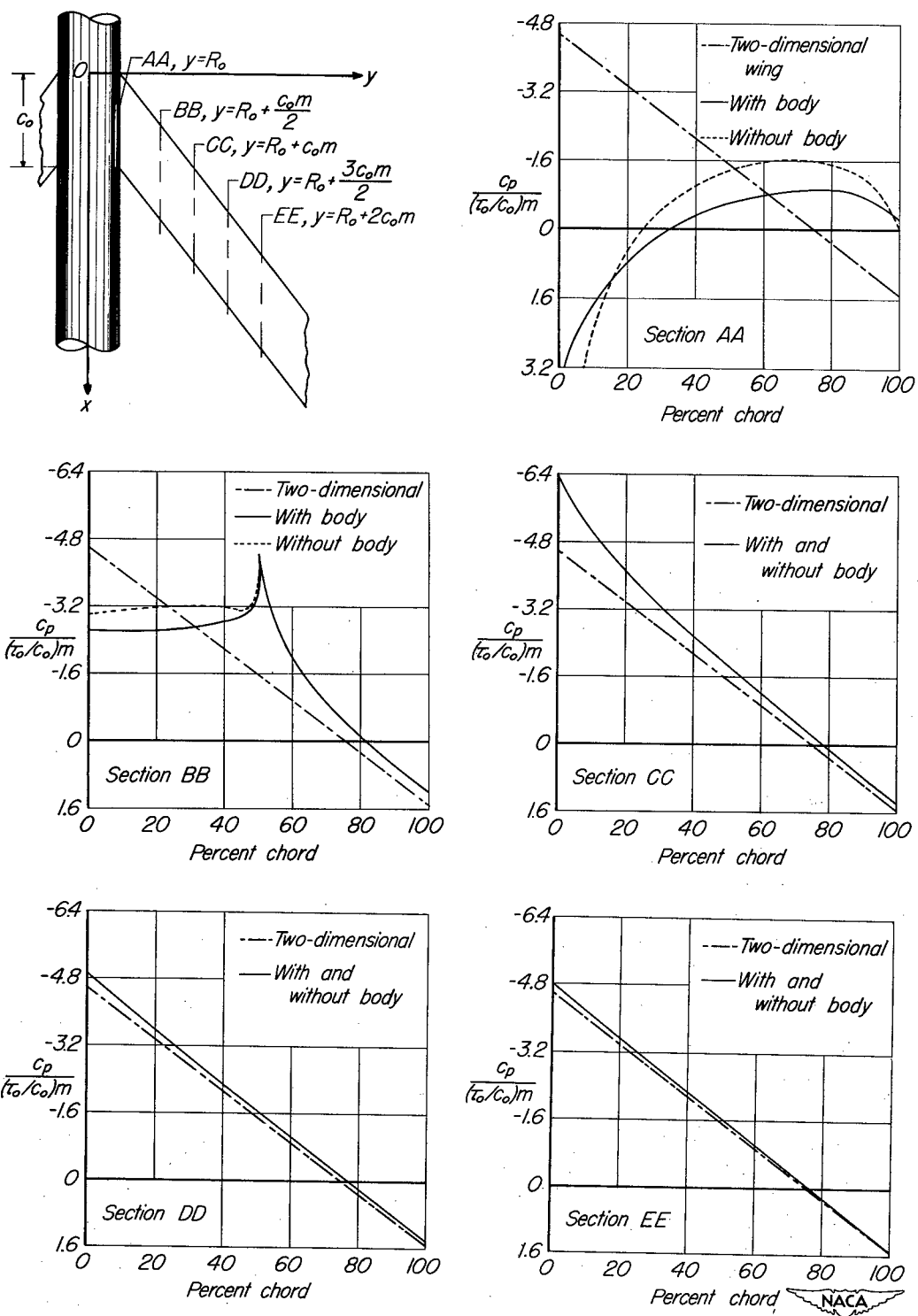


Figure 2.- Supersonic pressure coefficient on upper surface of wing of the basic combination;  $m\beta = 0.5$ .

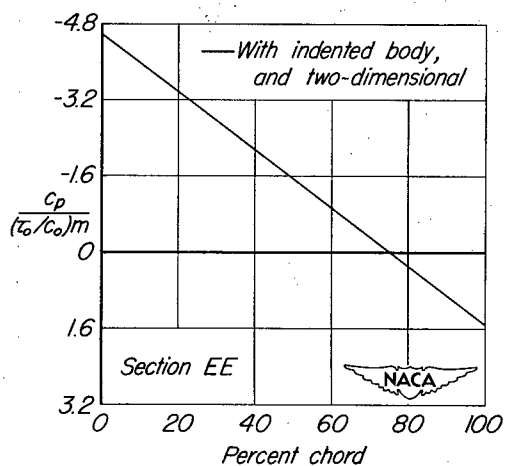
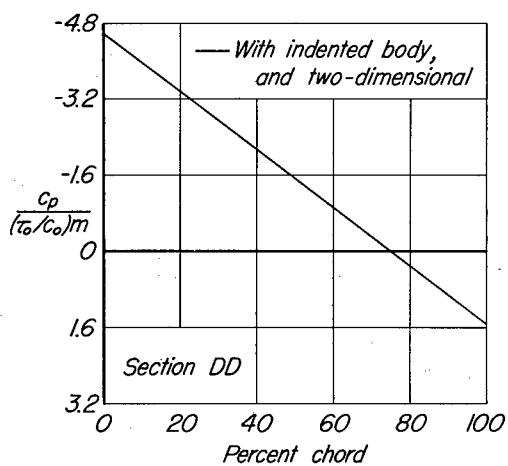
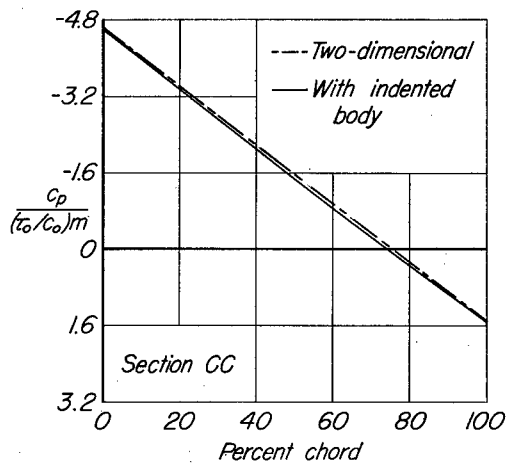
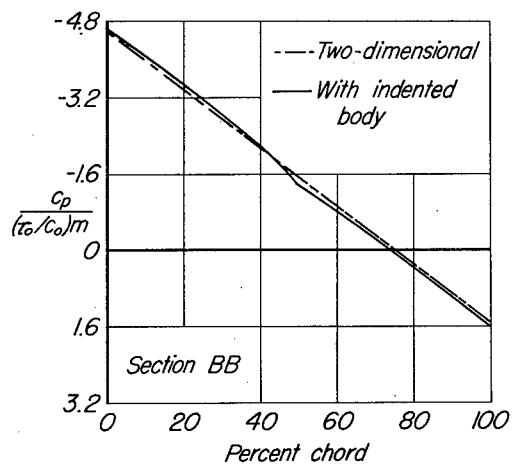
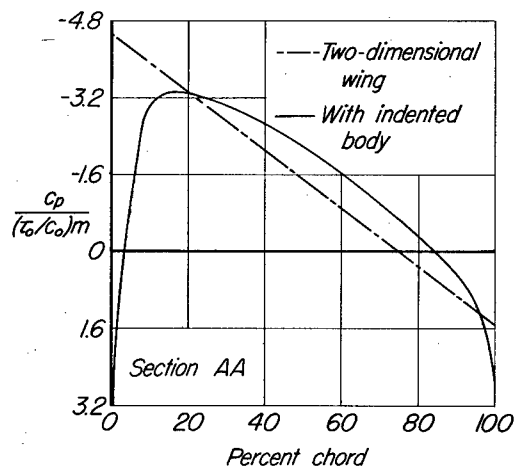
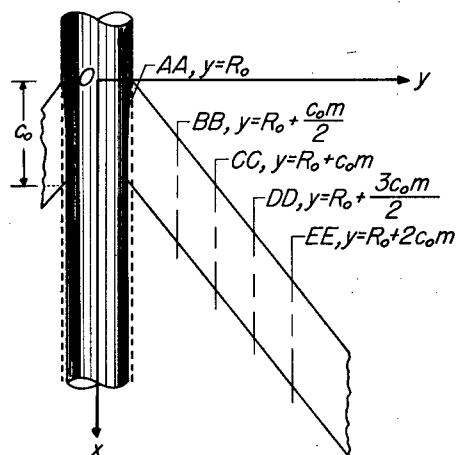


Figure 3.- Pressure coefficient on upper surface of wing of the indented wing-body combination.

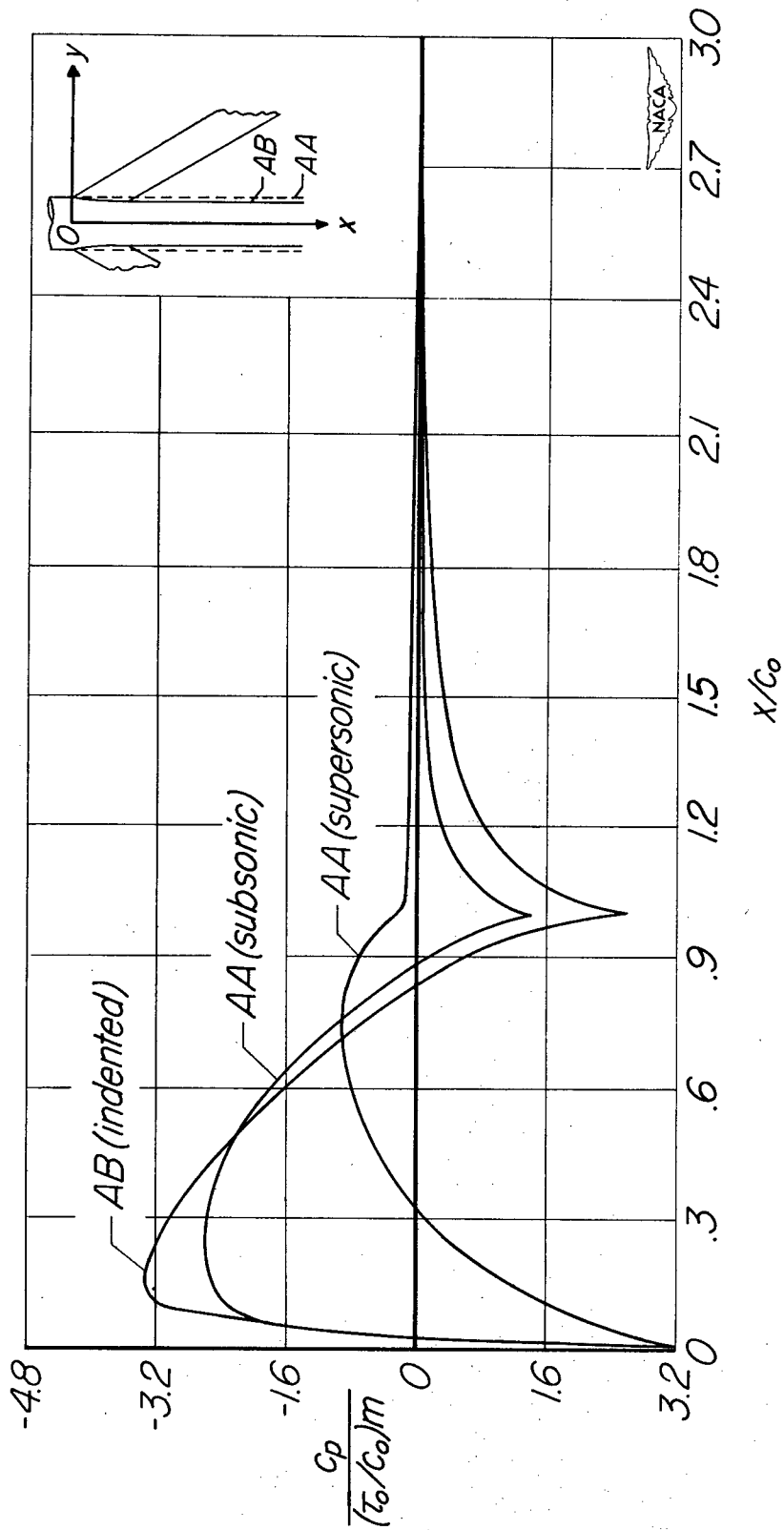
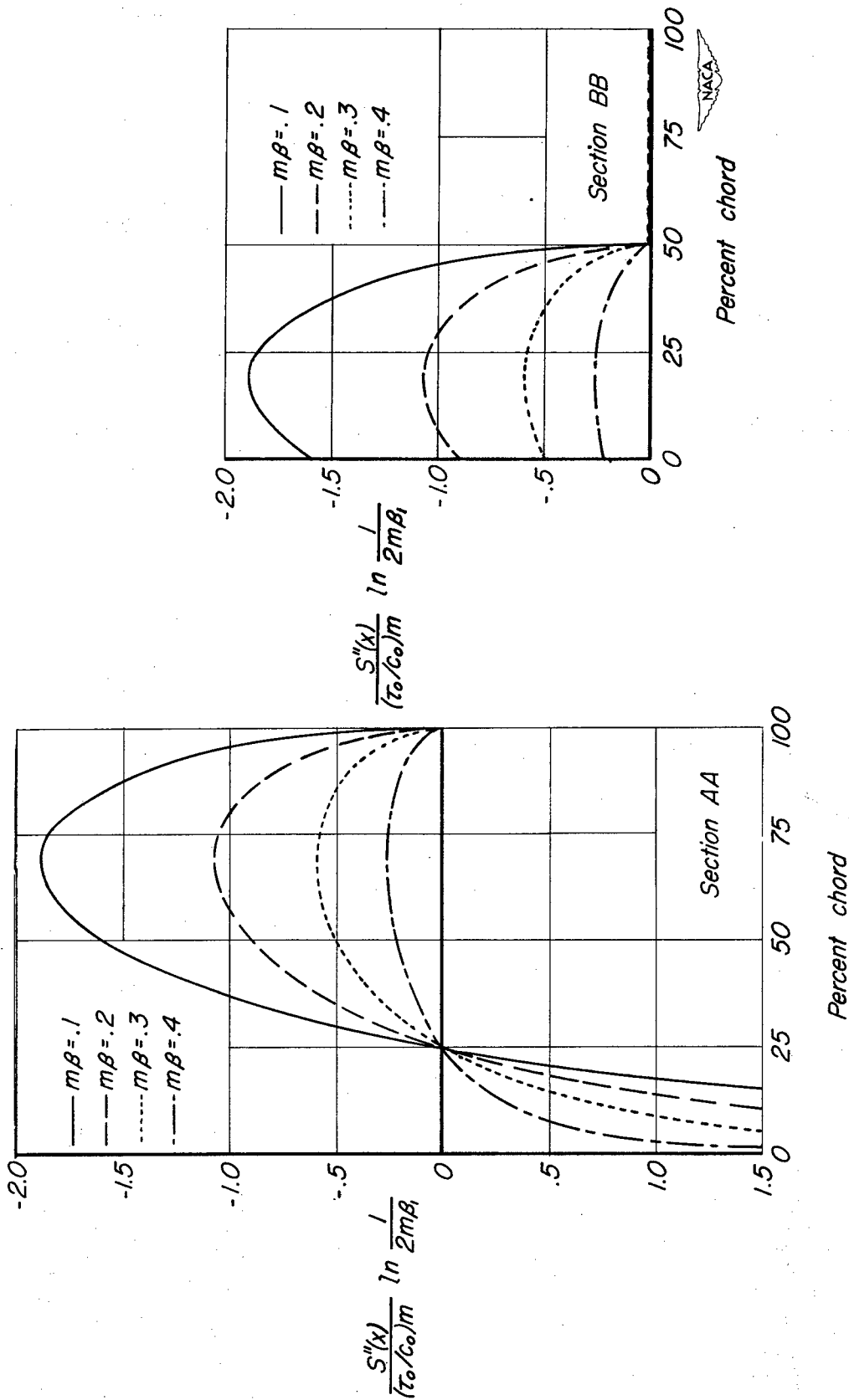
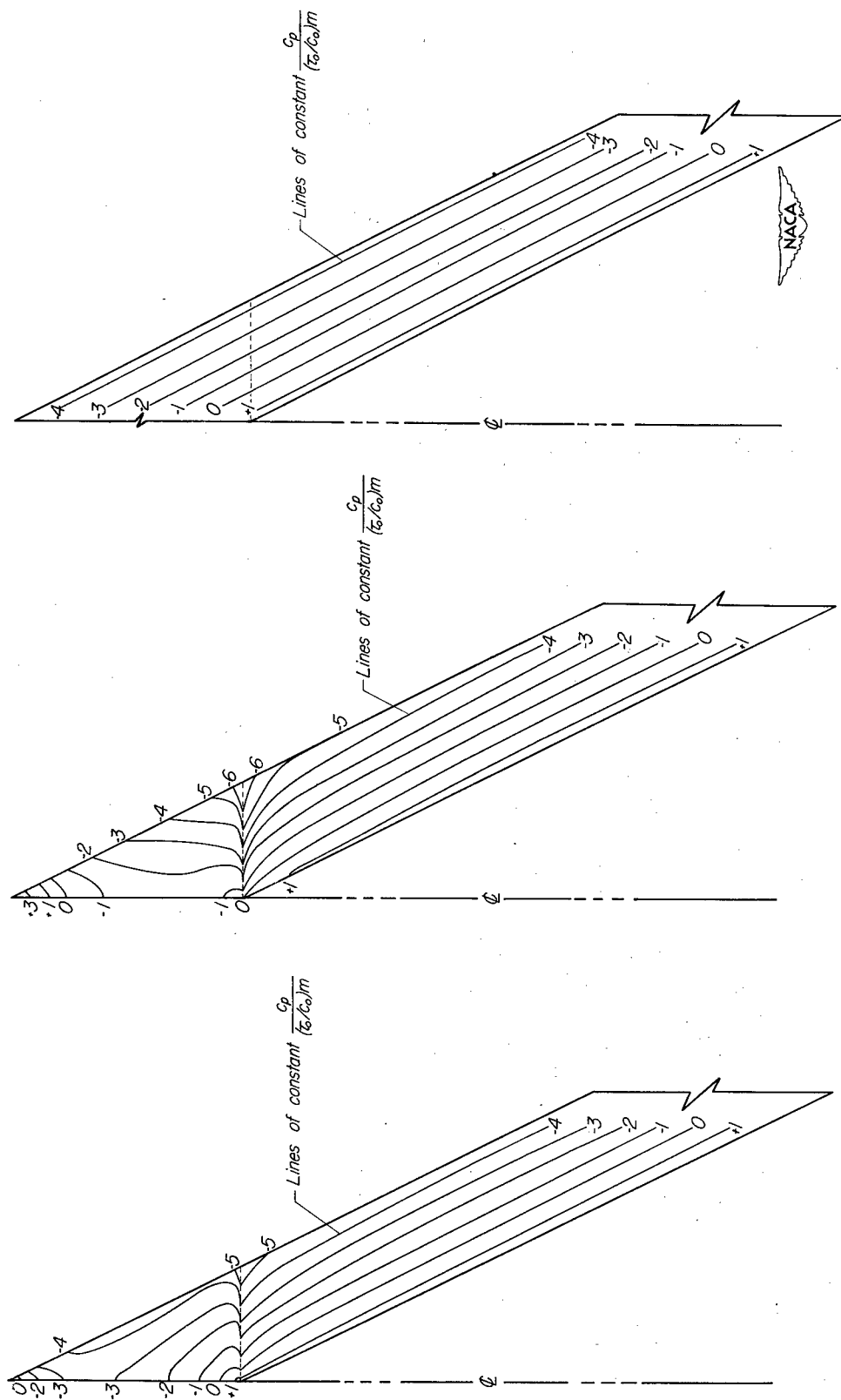


Figure 4.- Variation of pressure on the body in plane of wing;  $m\beta = 0.5$ .



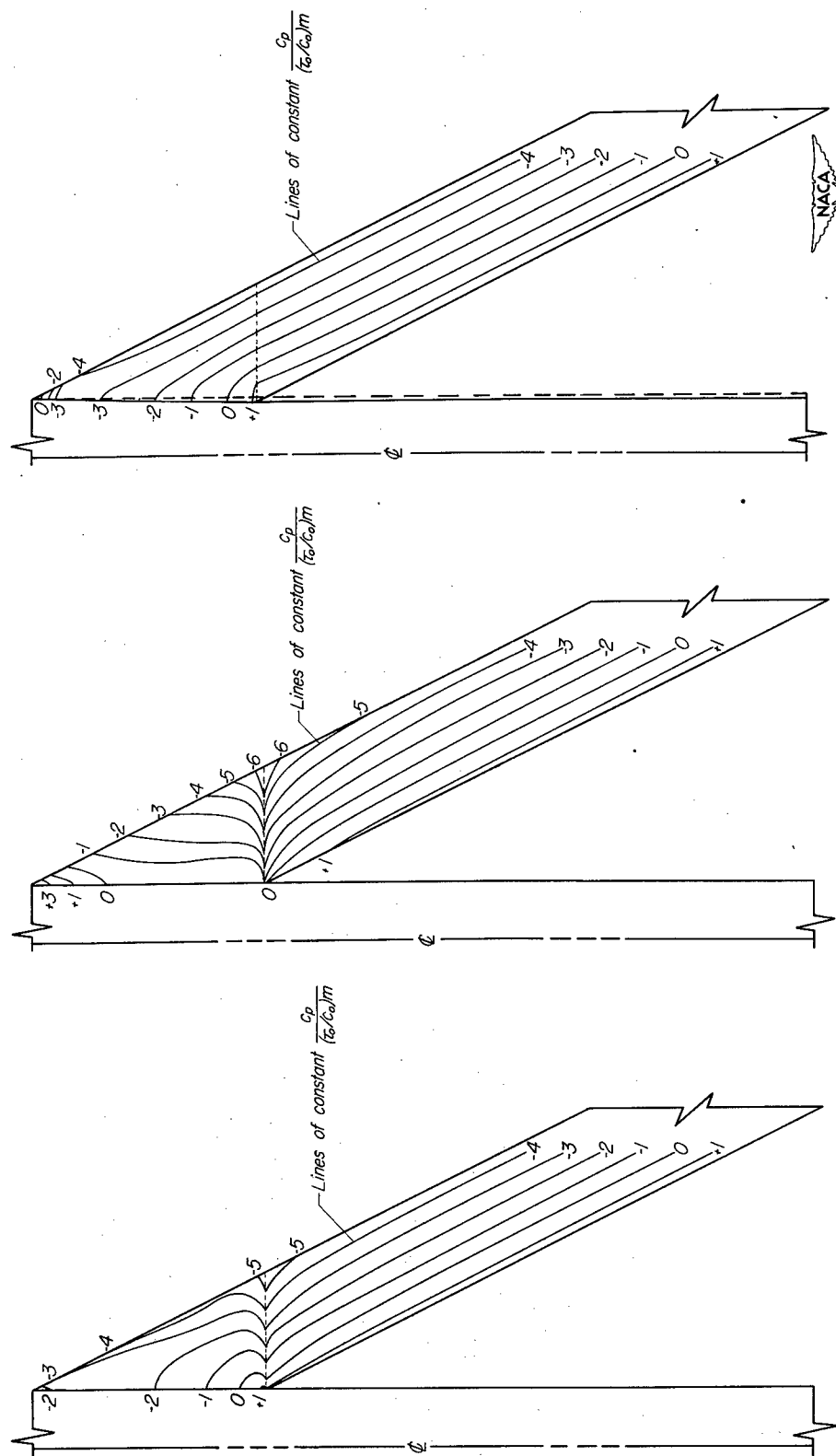
(a) For use with section AA of figures 1 and 2. (b) For use with section BB of figures 1 and 2.

Figure 5.- Function to be added to give values of pressure coefficient for other Mach numbers.



(a) Subsonic flow. (b) Supersonic flow. (c) Two-dimensional.




Figure 6.- Isobaric charts for the wing alone;  $m\beta = 0.5$ .



(a) Basic combination in subsonic flow. (b) Basic combination in supersonic flow. (c) Indented wing-body combination.

Figure 7.- Iso-baric charts for wing-body combinations;  $m\beta = 0.5$ .



<p>NACA TN 3674</p> <p>National Advisory Committee for Aeronautics.</p> <p>THEORETICAL PRESSURE DISTRIBUTIONS FOR SOME SLENDER WING-BODY COMBINATIONS AT ZERO LIFT. Paul F. Byrd. April 1956. 39p. diags. (NACA TN 3674. Supersedes RM A54J07)</p> <p>Theoretical calculations are made of the pressure distributions for some slender, symmetrical wing-body combinations in subsonic and supersonic flow. The combinations consist first of nonlifting, swept-back wings mounted on a circular cylinder and second of such wings mounted on a body indented so that the local cross-sectional area of the combination is constant. The results indicate that indentation straightens out the isobars along the wing and diminishes the maximum perturbation velocities.</p>	<p>1. Wings, Complete - Theory (1. 2. 2. 1)</p> <p>2. Wings, Complete - Sweep (1. 2. 2. 2. 3)</p> <p>3. Wing-Fuselage Combinations - Airplanes (1. 7. 1. 1. 1)</p> <p>4. Wing-Body Combinations - Missiles (1. 7. 2. 1. 1)</p> <p>I. Byrd, Paul F.</p> <p>II. NACA TN 3674</p> <p>III. NACA RM A54J07</p>	<p>NACA TN 3674</p> <p>National Advisory Committee for Aeronautics.</p> <p>THEORETICAL PRESSURE DISTRIBUTIONS FOR SOME SLENDER WING-BODY COMBINATIONS AT ZERO LIFT. Paul F. Byrd. April 1956. 39p. diags. (NACA TN 3674. Supersedes RM A54J07)</p> <p>Theoretical calculations are made of the pressure distributions for some slender, symmetrical wing-body combinations in subsonic and supersonic flow. The combinations consist first of nonlifting, swept-back wings mounted on a circular cylinder and second of such wings mounted on a body indented so that the local cross-sectional area of the combination is constant. The results indicate that indentation straightens out the isobars along the wing and diminishes the maximum perturbation velocities.</p>	<p>1. Wings, Complete - Theory (1. 2. 2. 1)</p> <p>2. Wings, Complete - Sweep (1. 2. 2. 2. 3)</p> <p>3. Wing-Fuselage Combinations - Airplanes (1. 7. 1. 1. 1)</p> <p>4. Wing-Body Combinations - Missiles (1. 7. 2. 1. 1)</p> <p>I. Byrd, Paul F.</p> <p>II. NACA TN 3674</p> <p>III. NACA RM A54J07</p>	<p>Copies obtainable from NACA, Washington</p>	
<p>NACA TN 3674</p> <p>National Advisory Committee for Aeronautics.</p> <p>THEORETICAL PRESSURE DISTRIBUTIONS FOR SOME SLENDER WING-BODY COMBINATIONS AT ZERO LIFT. Paul F. Byrd. April 1956. 39p. diags. (NACA TN 3674. Supersedes RM A54J07)</p> <p>Theoretical calculations are made of the pressure distributions for some slender, symmetrical wing-body combinations in subsonic and supersonic flow. The combinations consist first of nonlifting, swept-back wings mounted on a circular cylinder and second of such wings mounted on a body indented so that the local cross-sectional area of the combination is constant. The results indicate that indentation straightens out the isobars along the wing and diminishes the maximum perturbation velocities.</p>	<p>1. Wings, Complete - Theory (1. 2. 2. 1)</p> <p>2. Wings, Complete - Sweep (1. 2. 2. 2. 3)</p> <p>3. Wing-Fuselage Combinations - Airplanes (1. 7. 1. 1. 1)</p> <p>4. Wing-Body Combinations - Missiles (1. 7. 2. 1. 1)</p> <p>I. Byrd, Paul F.</p> <p>II. NACA TN 3674</p> <p>III. NACA RM A54J07</p>	<p>NACA TN 3674</p> <p>National Advisory Committee for Aeronautics.</p> <p>THEORETICAL PRESSURE DISTRIBUTIONS FOR SOME SLENDER WING-BODY COMBINATIONS AT ZERO LIFT. Paul F. Byrd. April 1956. 39p. diags. (NACA TN 3674. Supersedes RM A54J07)</p> <p>Theoretical calculations are made of the pressure distributions for some slender, symmetrical wing-body combinations in subsonic and supersonic flow. The combinations consist first of nonlifting, swept-back wings mounted on a circular cylinder and second of such wings mounted on a body indented so that the local cross-sectional area of the combination is constant. The results indicate that indentation straightens out the isobars along the wing and diminishes the maximum perturbation velocities.</p>	<p>1. Wings, Complete - Theory (1. 2. 2. 1)</p> <p>2. Wings, Complete - Sweep (1. 2. 2. 2. 3)</p> <p>3. Wing-Fuselage Combinations - Airplanes (1. 7. 1. 1. 1)</p> <p>4. Wing-Body Combinations - Missiles (1. 7. 2. 1. 1)</p> <p>I. Byrd, Paul F.</p> <p>II. NACA TN 3674</p> <p>III. NACA RM A54J07</p>	<p>Copies obtainable from NACA, Washington</p>	
<p>NACA TN 3674</p> <p>National Advisory Committee for Aeronautics.</p> <p>THEORETICAL PRESSURE DISTRIBUTIONS FOR SOME SLENDER WING-BODY COMBINATIONS AT ZERO LIFT. Paul F. Byrd. April 1956. 39p. diags. (NACA TN 3674. Supersedes RM A54J07)</p> <p>Theoretical calculations are made of the pressure distributions for some slender, symmetrical wing-body combinations in subsonic and supersonic flow. The combinations consist first of nonlifting, swept-back wings mounted on a circular cylinder and second of such wings mounted on a body indented so that the local cross-sectional area of the combination is constant. The results indicate that indentation straightens out the isobars along the wing and diminishes the maximum perturbation velocities.</p>	<p>1. Wings, Complete - Theory (1. 2. 2. 1)</p> <p>2. Wings, Complete - Sweep (1. 2. 2. 2. 3)</p> <p>3. Wing-Fuselage Combinations - Airplanes (1. 7. 1. 1. 1)</p> <p>4. Wing-Body Combinations - Missiles (1. 7. 2. 1. 1)</p> <p>I. Byrd, Paul F.</p> <p>II. NACA TN 3674</p> <p>III. NACA RM A54J07</p>	<p>NACA TN 3674</p> <p>National Advisory Committee for Aeronautics.</p> <p>THEORETICAL PRESSURE DISTRIBUTIONS FOR SOME SLENDER WING-BODY COMBINATIONS AT ZERO LIFT. Paul F. Byrd. April 1956. 39p. diags. (NACA TN 3674. Supersedes RM A54J07)</p> <p>Theoretical calculations are made of the pressure distributions for some slender, symmetrical wing-body combinations in subsonic and supersonic flow. The combinations consist first of nonlifting, swept-back wings mounted on a circular cylinder and second of such wings mounted on a body indented so that the local cross-sectional area of the combination is constant. The results indicate that indentation straightens out the isobars along the wing and diminishes the maximum perturbation velocities.</p>	<p>1. Wings, Complete - Theory (1. 2. 2. 1)</p> <p>2. Wings, Complete - Sweep (1. 2. 2. 2. 3)</p> <p>3. Wing-Fuselage Combinations - Airplanes (1. 7. 1. 1. 1)</p> <p>4. Wing-Body Combinations - Missiles (1. 7. 2. 1. 1)</p> <p>I. Byrd, Paul F.</p> <p>II. NACA TN 3674</p> <p>III. NACA RM A54J07</p>	<p>Copies obtainable from NACA, Washington</p>	

# NACA TN 3674

National Advisory Committee for Aeronautics.  
THEORETICAL PRESSURE DISTRIBUTIONS FOR  
SOME SLENDER WING-BODY COMBINATIONS AT  
ZERO LIFT. Paul F. Byrd. April 1956. 39p.  
diags. (NACA TN 3674. Supersedes RM A54J07)

Theoretical calculations are made of the pressure distributions for some slender, symmetrical wing-body combinations in subsonic and supersonic flow. The combinations consist first of nonlifting, swept-back wings mounted on a circular cylinder and second of such wings mounted on a body indented so that the local cross-sectional area of the combination is constant. The results indicate that indentation straightens out the isobars along the wing and diminishes the maximum perturbation velocities.

Copies obtainable from NACA, Washington

1. Wings, Complete - Theory (1. 2. 2. 1)
2. Wings, Complete - Sweep (1. 2. 2. 2. 3)
3. Wing-Fuselage Combinations - Airplanes (1. 7. 1. 1. 1)
4. Wing-Body Combinations - Missiles (1. 7. 2. 1. 1)
- I. Byrd, Paul F.
- II. NACA TN 3674
- III. NACA RM A54J07



# NACA TN 3674

National Advisory Committee for Aeronautics.  
THEORETICAL PRESSURE DISTRIBUTIONS FOR  
SOME SLENDER WING-BODY COMBINATIONS AT  
ZERO LIFT. Paul F. Byrd. April 1956. 39p.  
diags. (NACA TN 3674. Supersedes RM A54J07)

Theoretical calculations are made of the pressure distributions for some slender, symmetrical wing-body combinations in subsonic and supersonic flow. The combinations consist first of nonlifting, swept-back wings mounted on a circular cylinder and second of such wings mounted on a body indented so that the local cross-sectional area of the combination is constant. The results indicate that indentation straightens out the isobars along the wing and diminishes the maximum perturbation velocities.

Copies obtainable from NACA, Washington

1. Wings, Complete - Theory (1. 2. 2. 1)
2. Wings, Complete - Sweep (1. 2. 2. 2. 3)
3. Wing-Fuselage Combinations - Airplanes (1. 7. 1. 1. 1)
4. Wing-Body Combinations - Missiles (1. 7. 2. 1. 1)
- I. Byrd, Paul F.
- II. NACA TN 3674
- III. NACA RM A54J07

